Regimes of soil moisture-wet bulb temperature coupling with relevance to moist heat stress

Qinqin Kong[a] Matthew Huber[a]

[a] *Department of Earth, Atmospheric, and Planetary Sciences, Purdue University, West Lafayette, United States of America, 47907*

Corresponding author: Qinqin Kong, kong97@purdue.edu

Early Online Release: This preliminary version has been accepted for publication in *Journal of Climate*, may be fully cited, and has been assigned DOI 10.1175/JCLI-D-23-0132.1. The final typeset copyedited article will replace the EOR at the above DOI when it is published.

ABSTRACT: Human heat stress depends jointly on atmospheric temperature and humidity. Wetter soils reduce temperature but also raise humidity making the collective impact on heat stress unclear. To better understand these interactions, we use ERA5 reanalysis to examine the coupling between daily average soil moisture and wet-bulb temperature (T_w) and its seasonal and diurnal cycle at global scale. We identify a global soil moisture-T_w coupling pattern with both widespread negative and positive correlations in contrast to the well-established cooling effect of wet soil on dry-bulb temperature. Regions showing positive correlations closely resemble previously identified land-atmosphere coupling hotspots where soil moisture effectively controls surface energy partition. Soil moisture-T_w coupling varies seasonally closely tied to monsoon development, and the positive coupling is slightly stronger and more widespread during nighttime. Local-scale analysis demonstrates a nonlinear structure of soil moisture-T_w coupling with stronger coupling under relatively dry soils. Hot-days with high T_w values show wetter-than-normal soil, anomalous high latent and low sensible heat flux from a cooler surface, and a shallower boundary layer. This supports the hypothesis that wetter soil increases T_w by concentrating surface moist enthalpy flux within a shallower boundary layer and reducing free-troposphere air entrainment. We identify areas of particular interest for future studies on the physical mechanisms of soil moisture-heat stress coupling. Our findings suggest that increasing soil moisture might amplify heat stress over large portions of the world including several densely populated areas. These results also raise questions about the effectiveness of evaporative cooling strategies in ameliorating urban heat stress.

Accepted for publication in *Journal of Climate*. DOI 10.1175/JCLI-D-23-0132.1.

SIGNIFICANCE STATEMENT: The purpose of this study is to provide a global picture of the relationship between soil moisture anomalies and a heat stress metric that includes the joint effects of temperature and humidity. This is important because a better understanding of this relationship will help improve the prediction of extreme heat stress events and inform strategies for ameliorating heat stress. We find a wide-spread positive correlation between soil moisture and heat stress, in contrast to studies relying on temperature alone. This raises the possibility that, over much of the world, and in the most populous regions, strategies like irrigation or "greening" that can reduce temperature, might be ineffective or even harmful in reducing heat stress with humidity incorporated.

1. Introduction

Heat stress is a leading cause of weather-related fatalities (Buzan et al. 2015; Barriopedro et al. 2011) which is expected to increase in prevalence and intensity in the future (Diffenbaugh and Giorgi 2012; Sherwood and Huber 2010; Willett and Sherwood 2010). Heat stress in humans depends jointly on atmosphere dry-bulb temperature (T) and specific humidity (q) because heat storage in the body occurs when latent and sensible heat fluxes are insufficient to allow the body to balance its metabolic heat load (Wouters et al. 2022; Buzan and Huber 2020; Brunt 1943). The capability of the human body to cool via perspiration–the primary channel of heat dissipation for well-hydrated humans in hot environments–reduces strongly as atmospheric humidity increases.

Many studies investigated the physical processes that contribute to high T events, such as blocking (e.g., Neal et al. (2022); Brunner et al. (2018)), internal variability modes (e.g., Luo and Lau (2019); Parker et al. (2014)), and land-atmosphere interaction (e.g., Fischer et al. (2007); Miralles et al. (2014)). It is less clear to what extent these processes also control moist heat stress given the additional humidity dimension. Many different heat stress metrics that incorporate humidity exist and have various applications and relative strengths (Buzan et al. 2015; Ioannou et al. 2022). In this study, we focus on wet-bulb temperature (T_w) because of its straightforward meteorological and thermodynamic basis, and contrast it with the behavior of dry-bulb temperature.

As a starting point, it is useful to look at the spatio-temporal distribution of hot-days as defined by the familiar metric, dry-bulb temperature, and the temperature-humidity combined metric, T_w (see Section 2f for the definition of hot-days) and ask if these days coincide. If they do, then

Accepted for publication in *Journal of Climate*. DOI 10.1175/JCLI-D-23-0132.1.

there is little value added in studying the dynamics of moist separately from dry heat stress since the former would be a simple extension of the latter. However, it is clear that T- and T_w-defined hot-days overlap with each other by less than 30% across the tropics and subtropics and are nearly entirely separated (overlapping ratio<1%) over some monsoon regions (Fig. 1a). The overlapping ratio is less than 20% across half of the land area between 60°S and 70°N, and below 10% within half of the population (Fig. 1b). Lack of temporal overlap implies distinct physical processes controlling dry heat and moist heat (Ivanovich et al. 2022; Raymond et al. 2017; Monteiro and Caballero 2019) and motivates our exploration of moist heat stress dynamics as a distinct line of inquiry from the more traditional dry framework focusing mostly on dry-bulb temperature. The potential for distinctly different dynamics invites us to unravel the governing processes of humid heat in order to improve risk prediction and inform resilience and adaptation strategies.

This work focuses on one particular dimension of the governing processes of moist heat: how land surface moisture affects moist heat stress explicitly including the joint impact of atmospheric humidity and temperature changes. We are building on the large body of work on the relationship between soil moisture and near-surface air T from which a negative correlation has been established between soil moisture and T (Seneviratne et al. 2010). Soil moisture deficits are typically found to amplify hot T extremes both within historical events (e.g., Fischer et al. (2007); Miralles et al. (2014); Hauser et al. (2016)) and future projections in the context of climate change (e.g., Seneviratne et al. (2006); Vogel et al. (2017); Donat et al. (2017). Based on this conceptual model of strong evaporative cooling diminishing heat stress, evaporative cooling strategies (e.g., green roof and facades, urban water body, misting system, etc.) have been proposed to mitigate urban heat stress (Krayenhoff et al. 2018; Sharma et al. 2016; Aram et al. 2019; Völker et al. 2013). Expanding irrigation is considered to have ameliorated hot T exposure and benefited around a billion people (e.g., Cook et al. (2011); Lobell et al. (2008); Kueppers et al. (2007); Thiery et al. (2017)).

While the impact of enhanced surface moisture on T is well understood (Seneviratne et al. 2010), a global view of the net impact on heat stress including changes in atmospheric moisture content is not well established. Wetter soil partitions energy from sensible (SH) to latent heat flux (LH) (Seneviratne et al. 2010) which not only reduces T but also raises q making the collective impact on heat stress not self-evident. This leaves open the question of what the benefits of evaporative

Accepted for publication in *Journal of Climate*. DOI 10.1175/JCLI-D-23-0132.1.

cooling strategies are when both temperature and humidity are considered. Comparatively few evaluations have been conducted on the effectiveness of such strategies in terms of both T and q (Hu and Li 2020; Wang et al. 2022b; Lehnert et al. 2021). Results that appear superficially contradictory have been obtained regarding whether heat stress strengthens or weakens under wetter soil depending on whether only T is included versus a more complete accounting (Wouters et al. 2022; Mishra et al. 2020). A more complete analysis may resolve this apparent contradiction.

Many heat stress metrics have been developed that include moisture and weight temperature and humidity in different ways (de Freitas and Grigorieva 2015; Fiala and Havenith 2015; Buzan et al. 2015) and given the huge variety (more than 100) of such metrics it is not our goal in this study to revisit their relative merits in terms of formulation or empirical validation. Instead we chose to focus on those that have a sound thermodynamic basis and relatively simple convective and dynamical interpretative framework while still having a strong albeit imperfect relationship with the empirical heat stress literature (Foster et al. 2021). Several metrics match these criteria and have a straightforward first-principles basis including T_w (Sherwood and Huber 2010), equivalent potential temperature (θ_e) (Song et al. 2022), and moist enthalpy or equivalent temperature (Matthews et al. 2022). These all reflect moist static energy (MSE) and are essentially equivalent given appropriate assumptions (Sherwood and Huber 2010; Zhang et al. 2021; Raymond et al. 2021; Buzan and Huber 2020). In that sense, understanding the controls and behavior of one of these metrics will provide general insights into any of them and other more empirical metrics which depend on the same underlying physics (Vecellio et al. 2022). In this study we attempt to understand the physical interactions between soil moisture and heat stress as measured by near-surface T_w.

Despite the clearly established cooling impact of enhanced evaporation on dry heat stress, the opposite may be true for moist heat stress, at least some of the time. For example, some earlier studies on soil moisture-precipitation coupling detected higher afternoon boundary layer (PBL) θ_e or MSE conditioned on wetter soil in the morning in local field observations (Betts and Ball 1995, 1998; Eltahir 1998), as supported by modeling studies (Pal and Eltahir 2001; Zheng and Eltahir 1998; Findell and Eltahir 2003a,b; Schär et al. 1999). Other observational research in Illinois however did not find a significant correlation between soil moisture and T_w (Findell and Eltahir 1999). A more recent observational campaigns over southeastern Nebraska, the Great Plains Irrigation Experiment (GRAINEX), found higher daytime peak θ_e over irrigated than non-

Accepted for publication in *Journal of Climate*. DOI 10.1175/JCLI-D-23-0132.1.

irrigated sites (Rappin et al. 2021). Using reanalysis data, recent studies identified a higher T_w (up to 2.5 °C) over irrigated area than the surroundings in Saudi Arabia (Safieddine et al. 2022), a temporal clustering of high T_w days around precipitation events in arid region (Speizer et al. 2022), and an amplification of urban heat stress by expanding irrigation over northern India (Guo et al. 2022), all of which suggest a positive relation between soil moisture and heat stress. Modeling experiments also found a heat stress amplification by irrigation (Kang and Eltahir 2018; Krakauer et al. 2020; Mishra et al. 2020) with the magnitudes depending on the chosen heat stress metrics (Mishra et al. 2020) since different metrics weight humidity differently. Improvement in irrigation efficiency was found to reduce heat stress (Ambika and Mishra 2022).

Previous studies on soil moisture-precipitation coupling sketch the physical pathway linking soil moisture to PBL θ_e (or MSE, or T_w) as: (1) wetter soil enhances both net solar and terrestrial radiation at surface by lowering albedo and cooling the surface; (2) the re-partition of surface radiative energy from SH to LH under wet soil reduces surface buoyancy flux which curtails entrainment of low moist entropy air from free troposphere; (3) less free troposphere air entrainment suppresses PBL growth leading to a concentration of surface heat flux input within a shallower PBL (Findell and Eltahir 2003a; Eltahir 1998; Pal and Eltahir 2001). These three factors are additive and collectively raise PBL θ_e and T_w.

Despite existing observational or reanalysis-based evidence of soil moisture-heat stress coupling at local or regional scale, a global picture is absent and it is unclear whether the coupling sign is uniform globally and where the coupling strength is particularly strong. How this coupling varies seasonally and diurnally is also poorly constrained in a global sense. In addition, the extent the physical mechanism linking wetter soil to stronger heat stress as described above is supported by observations or reanalysis has not been demonstrated. This study fill these gaps by investigating soil moisture-T_w (SM-T_w) coupling and its seasonal and diurnal cycle at global scale using ERA5 reanalysis data (Hersbach et al. 2020; Bell, B. et al. 2020). We also examine whether the covariations in T_w, soil moisture, surface turbulent and radiative fluxes, and PBL depth (PBLH) are consistent with the aforementioned physical mechanism.

The remainder of this paper is organized as follows. Section 2 describes the data and methodology. Results are then presented in Section 3 including: the global distribution of SM-T_w coupling in summer (Section 3a), the seasonal (Section 3b) and diurnal (Section 3c) variation in SM-T_w

Accepted for publication in *Journal of Climate*. DOI 10.1175/JCLI-D-23-0132.1.

coupling, and a detailed investigation on the nonlinear SM-T_w coupling structure within several selected local regions (Section 3d). To confirm that these findings are robust to methodological choices including sampling strategy and statistical coupling quantification, we adopt a different sampling method focusing only on hot-days with extremely high T_w values, and compute the composite anomalies conditioned on hot-days in Section 3e. Section 4 includes discussions on the comparison between our results and findings from prior work, limitations of this study and future research opportunities. Finally, Section 5 contains a brief summary and practical implications of our results.

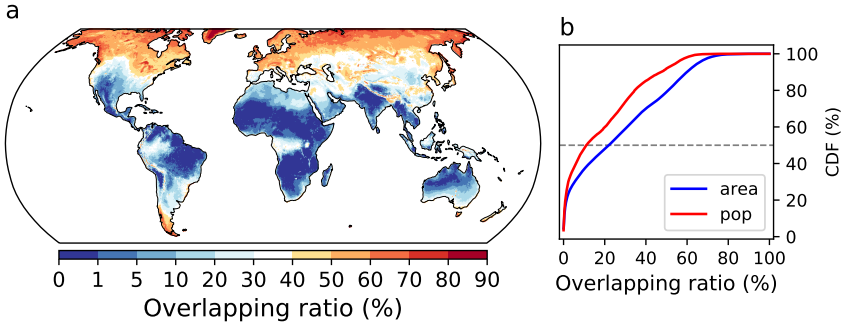

FIG. 1. Overlap ratio between T- and T_w-defined hot-days during 1950-2019: (a) the spatial distribution, and (b) the area- and population-weighted empirical cumulative distribution function (CDF) for land grid cells between 60°S and 70°N. Low overlap values indicate extremes of moist and dry heat stress do not co-occur and may therefore have different synoptic settings and dynamical controls.

2. Data and Methods

a. Data source

This study investigates the coupling between soil moisture and T_w and their covariation with surface temperature (T_s), surface turbulent and radiative fluxes, PBLH and 500-hPa geopotential height (Z500). To study the interaction of these variables, we use ERA5 reanalysis data on an hourly-basis at a spatial resolution of $0.25° \times 0.25°$ covering the period 1950-2019 (Hersbach et al. 2020; Bell, B. et al. 2020). While many different observational products could be used for investigating soil moisture or temperature separately and each has its own strengths, we are especially interested in having a homogeneous global coverage of all the relevant variables simultaneously.

Accepted for publication in *Journal of Climate*. DOI 10.1175/JCLI-D-23-0132.1.

Reanalysis products have global coverage and spatial continuity compared with pointwise in-situ measurements which are sparse and spatially uneven—especially for soil moisture. In addition, all required variables are available within reanalysis archives which ensures physical consistency among different quantities.

ERA5 is a state-of-art reanalysis product, with substantial improvements over earlier, similar products. Compared with its predecessor ERA5-interim, ERA5 adopts the HTESSEL land surface scheme with revised hydrology (Balsamo et al. 2015) and an improved land data assimilation system (de Rosnay et al. 2014). It also assimilates remote sensing soil moisture products and adopts more accurate boundary conditions of soil texture and monthly-varying vegetation (Balsamo et al. 2009; Boussetta et al. 2013). The combination of these changes contributes to significant improvements in the soil moisture and land surface fluxes consistency (Hersbach et al. 2020). ERA5 has a four-layer representation of soil, and the first-layer (0 - 7cm below the surface) soil moisture is used in this study.

It has been shown that ERA5 has considerable fidelity in representing the monthly dynamics and spatial structure of the observed soil moisture variations (except over parts of the high latitudes and regions with complex topography), and outperforms other reanalysis products in simulating soil moisture and evapotranspiration (ET) (Li et al. 2020b; Yang et al. 2021, 2022; Mahto and Mishra 2019). A joint evaluation on ERA5 soil moisture and temperature showed physically consistent water-heat balances with observed precipitation and near-surface air temperature (Li et al. 2020b). ERA5 was also demonstrated to be able to suitably capture the nonlinear coupling structure between soil moisture and extreme T (Benson and Dirmeyer 2021).

ERA5 or other reanalysis products are still faced with substantial biases in absolute soil moisture levels, and have difficulty in reproducing observed long-term trends in soil moisture (Li et al. 2020b; Yang et al. 2022; Mahto and Mishra 2019). This is less a concern in our study since we focus on the short-term covariation between soil moisture and other quantities with mean values and long-term trends removed.

To highlight the exposure of people to the potentially hazardous SM-T_w coupling regimes identified in this study, we weight the results by gridded world population data (GPWv4.11) Center for International Earth Science Information Network - CIESIN - Columbia University (2018) for year 2020 with a spatial resolution of $0.25° \times 0.25°$.

Accepted for publication in *Journal of Climate*. DOI 10.1175/JCLI-D-23-0132.1.

b. Wet-bulb temperature calculation

The heat stress metric we adopt is T_w which is the temperature an air parcel would attain if water is evaporated into the air to the point of saturation with all latent heat supplied by the parcel (Bohren and Albrecht 1998). T_w was used to set an upper limit for human thermal tolerance (Sherwood and Huber 2010; Haldane 1905) and has been widely used for quantifying heat stress in recent years (Raymond et al. 2020; Coffel et al. 2018, 2019; Pal and Eltahir 2016; Im et al. 2017; Li et al. 2020a).

T_w is essentially a measure of moist enthalpy which is defined as follows: $C_pT + L_vq$ (Raymond et al. 2021; Eltahir and Pal 1996), where C_p is the specific heat of air at constant pressure, and L_v is the latent heat of vaporization. The isobaric formulation of T_w changes at the same rate in response to perturbations in sensible (C_pT) and latent heat (L_vq): $\frac{\partial T_w}{\partial C_pT} = \frac{\partial T_w}{\partial L_vq}$ (see derivations in the Appendix). This study adopts the Davies-Jones adiabatic T_w formulation (Davies-Jones 2008; Buzan et al. 2015) which generates values very close to the isobaric formulation at constant pressure, but is more general. Both formulations have been widely used in heat stress literature (e.g., Li et al. (2020a) and Zhang et al. (2021) for isobaric T_w; Raymond et al. (2020), Coffel et al. (2018), and Im et al. (2017) for adiabatic T_w) and are substantially more accurate than more approximate forms (Buzan and Huber 2020), including the oft-used Stull approximation. ERA5 2-meter air and dewpoint temperature and surface pressure are used here for calculating T_w.

In addition to the strong meteorological theoretical basis for using T_w, as described further below, T_w also comprises approximately 70% of wet-bulb globe temperature (WBGT). WBGT is a widely-used, highly validated empirical heat stress measure (Ioannou et al. 2022; Kong and Huber 2022), so understanding T_w dynamics should provide some insights into the drivers of heat stress-related health, labor, and economic impacts (Saeed et al. 2022).

c. Statistical sampling method

Analyses in this study are based on daily anomalies unless otherwise mentioned. Anomalies are calculated for each day as deviations from climatological values. The climatological values are computed for each date by averaging over a 3-day moving window across a 31-year moving interval. For example, the climatology value for July 15, 2000 is calculated as the average over July 14-16 across 1985-2015. This sampling strategy removes both the seasonal cycle and secular trend

Accepted for publication in *Journal of Climate*. DOI 10.1175/JCLI-D-23-0132.1.

due to climate change which could otherwise distort the coupling quantification. The 3-day moving window is adopted to increase the sample size (93 days) from which we obtain the climatological values, and we have explored sensitivity to the moving window width and found our results are robust.

Soil moisture's control on surface energy partition and PBL growth is more relevant during daytime with solar heating. Wetter soil may correspond to anomalous cool surface and shallow PBL during daytime, but warm surface and deep PBL during nighttime possibly due to moisture limiting surface longwave cooling (Raymond et al. 2021). To avoid blending daytime and nighttime anomalies of opposite signs, we calculate anomalies for daytime average T_s, surface turbulent and radiative fluxes and PBLH, and whole-day average T, q, T_w, soil moisture and Z500.

d. Coupling metric

Coupling strength is measured with the sensitivity index (I) developed by Dirmeyer (2011) which has been frequently applied for quantifying land-atmosphere coupling (e.g., Giles et al. (2023); Li et al. (2022); Wei and Dirmeyer (2012)). To calculate the coupling between soil moisture and T_w, the index I_{SM-T_w} is formulated as the product between the slope of a linear regression of T_w against soil moisture and the standard deviation of soil moisture. The generated value indicates T_w changes per standard deviation increases in soil moisture (hereafter designated as $°C/\sigma_{SM}$). The coupling between other pairs of quantities is quantified and denoted in the same way. The statistical significance of the sensitivity index is evaluated with a two-tailed Wald test using the Scipy Python package (Virtanen et al. 2020).

e. Seasonal and diurnal cycle

The seasonal and diurnal cycle of SM-T_w coupling are relevant for this study. For the seasonal cycle, we first quantify SM-T_w coupling within summer which is defined for each grid cell as the hottest three calendar months in terms of climatological (1950-2019) monthly mean T_w (Fig. S1). Afterwards, we calculate I_{SM-T_w} for each calendar month separately and examine its temporal variation over the course of the year. The diurnal cycle is investigated by calculating I_{SM-T_w} from anomalies in daily average soil moisture (given its relatively small diurnal variability) and T_w of each hour of the day within local summer. Hourly anomalies are computed in the same way as

Accepted for publication in *Journal of Climate*. DOI 10.1175/JCLI-D-23-0132.1.

daily anomalies albeit conditioned on hour of the day. We also repeat the calculation with T_w and soil moisture anomalies of both hourly scale, and the results are nearly identical (not shown).

f. Hot-days composite analysis

SM-T_w coupling is first quantified via calculating the coupling metric as described above from all days within the selected season. To confirm that our findings are robust to methodological choices on sampling strategy and statistical coupling quantification, we then only sample hot-days and compute the composite anomalies in soil moisture conditioned on these hot-days. Hot-days are defined as days with daily maximum T_w exceeding the 90th percentile of its empirically determined distribution in summer across a 31-year window. To complement these analyses, we also examine the composite anomalies of several other land surface and atmospheric quantities including T and q, SH and LH, T_s, PBLH, surface downward solar radiation and Z500. The aim is to investigate whether these quantities exhibit coherent behaviors consistent with the physical mechanisms behind soil moisture-heat stress coupling proposed by previous studies (e.g., wetter soil, cooler surface, anomalous high LH and low SH, and shallower PBL conditioned on hot-days). A sign test is performed to evaluate the extent to which the signal is consistent among hot-days by calculating the percentage of hot-days having anomalies of the same sign as the composite anomaly for each grid cell. We highlight grid cells where the percentage exceeds 2/3 which is beyond the 99.99th percentile of the distribution from a binomial process with the same number of draws as hot-day frequencies and equal chances of positive or negative outcomes. The sign test is robust to events with anomalies of large magnitudes which could dominate a mean-value t-test (Pozo-Vázquez et al. 2005; Kiladis and Diaz 1989).

3. Results

a. Global distribution of SM-T_w coupling in summer: identification of hotspots and regimes

SM-T_w coupling is first examined in summer (as defined in methods Section 2e). To confirm that our methodological choices and data produce results that comport with prior work, we start by showing a globally negative correlation between daily average soil moisture and T (Fig. 2a). This result is consistent with the well-acknowledged cooling effect of wet soil by re-partitioning energy from SH to LH (Seneviratne et al. 2010), and aligns with expectation for the relationship between

Accepted for publication in *Journal of Climate*. DOI 10.1175/JCLI-D-23-0132.1.

soil moisture and heat stress as measured by dry metrics (Thiery et al. 2017, 2020). Although wet soil cools T globally (with the exception of deserts), it enhances q only over parts of the land area with statistically insignificant or even negative I_{SM-L_vq} over the high latitudes and parts of the tropics (Fig. 2b). This will be discussed later in this section. Consistent with temperature reduction and/or specific humidity enhancement, wet soil raises relative humidity (RH) globally (Fig. 2c).

The enhancement in latent heat with increasing soil moisture outweighs the reduction in sensible heat over some regions. This creates a complex structure of I_{SM-T_w} comprised by both positive and negative values (Fig. 2d) in contrast with the uniform negative correlation between soil moisture and temperature. I_{SM-T_w} is statistically significant positive over several regions such as Southwest North America, the Sahel zone, south and east Africa, the Indus Valley and Australia. These regions are referred to as SM-T_w coupling hotspots throughout the paper (Fig. 2d). As soil moisture increases in these regions, C_pT declines by 0.5-2.5 kJ/kg/σ_{SM} (equivalent to a temperature decrease of 0.5-2.5°C/σ_{SM}), but L_vq rises by 2.5-7.0 kJ/kg/σ_{SM} leading to a net increase in T_w of 0.6-1.5°C/σ_{SM}. Replacing daily average T_w with daily maximum values barely changes the pattern (not shown). This pattern is robust to statistical method choices: the spatial distributions of the Pearson and Kendall rank correlation between soil moisuture and T_w (Fig. S2) closely resemble the pattern in figure 2d.

The distributions of SM-T_w coupling hotspots coincides with regions with a significant positive relation between soil moisture and LH (Fig. 2d, e). These regions have been previously identified as land-atmosphere coupling hotspots (Koster 2004; Koster et al. 2006; Miralles et al. 2012; Dirmeyer 2011) where soil moisture varies substantially due to precipitation variability and acts as the limiting factor for ET (i.e., transitional ET regime). In this transitional ET regime, soil moisture can effectively control surface energy partition with more energy partitioned towards LH under wetter soil (Seneviratne et al. 2010). However, the surface energy re-partition alone cannot explain the relatively muted reduction of sensible heat compared with the latent heat increase and the net enhancement of T_w. The subsequent boundary layer response is needed to close the logic gap. The re-partition of energy from SH to LH under wet soil (Fig. 2e) generates a shallower PBL (Fig. 2f) over SM-T_w coupling hotspots which traps surface enthalpy flux into a smaller volume. This tends to mute the cooling and enlarge the moistening effect. The reduction of dry air entrainment

Accepted for publication in *Journal of Climate*. DOI 10.1175/JCLI-D-23-0132.1.

may further contribute to a stronger increase in latent heat (van Heerwaarden et al. 2009). This is consistent with the proposed physical mechanism associating wetter soil with stronger heat stress (namely wet soil suppresses PBL growth and cuts off the entrainment of free-troposphere air).

A weak or even negative SM-T_w coupling is identified over northern high latitudes and the tropics (Fig. 2d and Fig. S2). This type of relationship has been proposed to be due to the fact that ET over these regions is limited by solar radiation instead of soil moisture (Teuling et al. 2009) under which cases soil moisture variations are driven by changes in ET rather than the other way around (Wei and Dirmeyer 2012). Our results support this interpretation given the negative I_{SM-LH} and positive $I_{LH-PBLH}$ values (Fig. 2e, f). Without effective control of soil moisture on ET, specific humidity becomes insensitive to soil moisture variation (Fig. 2b). Wet soil is associated with weak surface ET (and weak SH) as a result of less incoming solar radiation which generates a lower T_w.

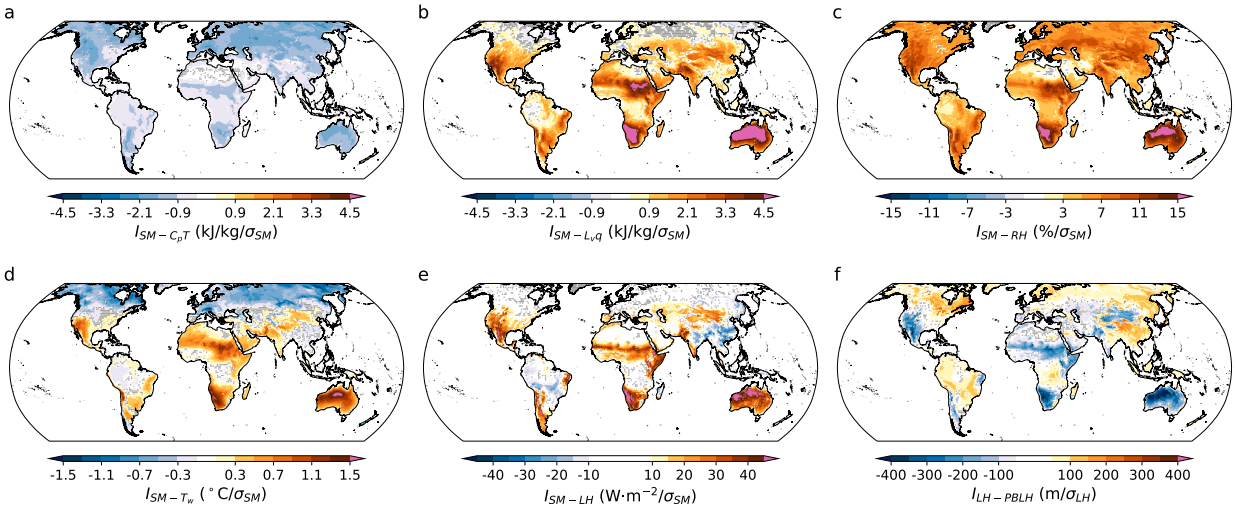

FIG. 2. Sensitivity indexes: (a) I_{SM-C_pT}, (b) I_{SM-L_vq}, (c) I_{SM-RH}, (d) I_{SM-T_w}, (e) I_{SM-LH} and (f) $I_{LH-PBLH}$. The calculations are based on anomalies of daily average soil moisture, T, q and T_w, and daytime average LH and PBLH during summer of 1950-2019. T and q are scaled by C_p and L_v to ensure the same unit. Surface heat fluxes are positive upwards. Stipples signify regions of statistical insignificance at 0.1% level.

b. Seasonal variations in SM-T_w coupling

In the previous section, we identified regions with significant positive SM-T_w coupling in summer. But dangerous heat stress is possible during periods other than the hottest three months–such as over the tropics and subtropics–in which case a significant positive I_{SM-T_w} may also indicate an

Accepted for publication in *Journal of Climate*. DOI 10.1175/JCLI-D-23-0132.1.

amplification of health-endangering heat stress under wet soil. Therefore, we need to broaden the study beyond summer and include analysis of the seasonal cycle of SM-T_w coupling which is expected to vary seasonally given its strong dependence on the general circulation and regional climate features. As shown in figure 3, the distribution of I_{SM-T_w} varies over the course of the year broadly following the I_{SM-LH} pattern (Fig. S3) which is related to the seasonal variations in precipitation and solar radiation.

The SM-T_w coupling hotspots generally have monsoonal climates where I_{SM-T_w} follows the swing of monsoon rain belts. For example, I_{SM-T_w} tracks the northward march of the ITCZ within the West African Monsoon region (Zhang and Wang 2008) with high values over the northern edge of the rain band centering the 0.5 mm/day isoline where large I_{SM-LE} values also reside (Fig. 4). As seen in figure 4b, the monsoon precipitation band moves poleward in conjunction with, and just south of, the maximum of T_w. These results show the linkages between the maximum T_w (equivalent to sub-cloud layer θ_e) and seasonal shifts in the peak monsoonal precipitation expected from convective quasi-equilibrium theory under angular momentum constraints (Nie et al. 2010; Emanuel 1995) which are also seen in other monsoonal regions (Acosta and Huber 2020). The implication is that moist heat stress in this region is intimately tied up with the dynamics of the moisture modulated seasonal shifts of the Saharan shallow meridional circulation which is part of the overall West African monsoon(Shekhar and Boos 2017).

Over the North American Monsoon region (Zhang and Wang 2008), I_{SM-T_w} becomes significantly positive at Mexico in May which then strengthens and expands northward to the southwest United States from June to September as the monsoon develops (Fig. 3e-i). Australia and South Africa show significant positive I_{SM-T_w} during large portion of the year with peak values in austral summer (Fig. 3). Over the Indus Valley, significant positive I_{SM-T_w} first occurs in June and then strengthens during July to September which coincides with the local monsoon season (Fig. 3f-i). The climatologically wet areas of the Indian subcontinent, in contrast, show significant positive I_{SM-T_w} during pre- (Mar-May) and post-monsoon (Oct-Nov) seasons (Fig. 3c-e and j-k). The monsoon season (Jul-Sep) is characterized by energy-limited ET regime showing negative I_{SM-LE} (Fig. S3g-i) and weak I_{SM-T_w} values (Fig. 3g-i).

By looking at the seasonal cycle of SM-T_w coupling, it is possible for regions other than the SM-T_w coupling hotspots to have a significant positive relation between soil moisture and T_w.

Accepted for publication in *Journal of Climate*. DOI 10.1175/JCLI-D-23-0132.1.

The positive coupling occurs during periods outside of local summer yet severe heat stress is still possible. Some examples are central Africa and Brazil from May to September and India during pre- and post-monsoon seasons when the monthly 99th percentile of T_w is well beyond 20°C and can reach up to more than 28 °C (Fig. S4).

Seasonal variations in SM-T_w coupling suggests that the impact of land use and land management practices such as irrigation on heat stress is sensitive to the period of year under consideration. Assessments on such impact should account for potential seasonal differentiation (Xu et al. 2015; Lejeune et al. 2017). When assessing the impact of irrigation on heat stress, it is important to be aware of local irrigation season and the season of severe heat stress in order for the results to be more realistic and practically useful (Guo et al. 2022; Mishra et al. 2020; Jha et al. 2022).

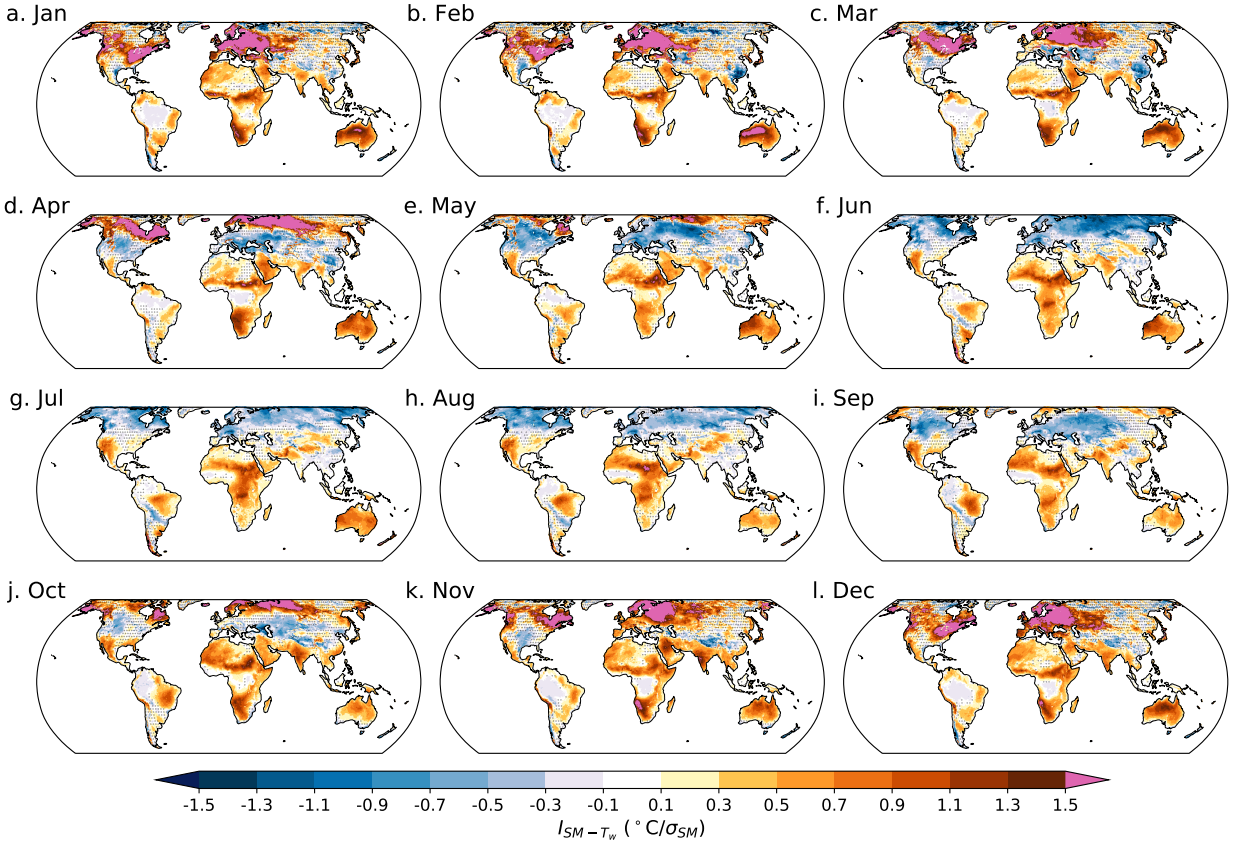

FIG. 3. Sensitivity index I_{SM-T_w} for each calendar month during 1950-2019. Stipples signify regions of statistical insignificance at 0.1% level.

Accepted for publication in *Journal of Climate*. DOI 10.1175/JCLI-D-23-0132.1.

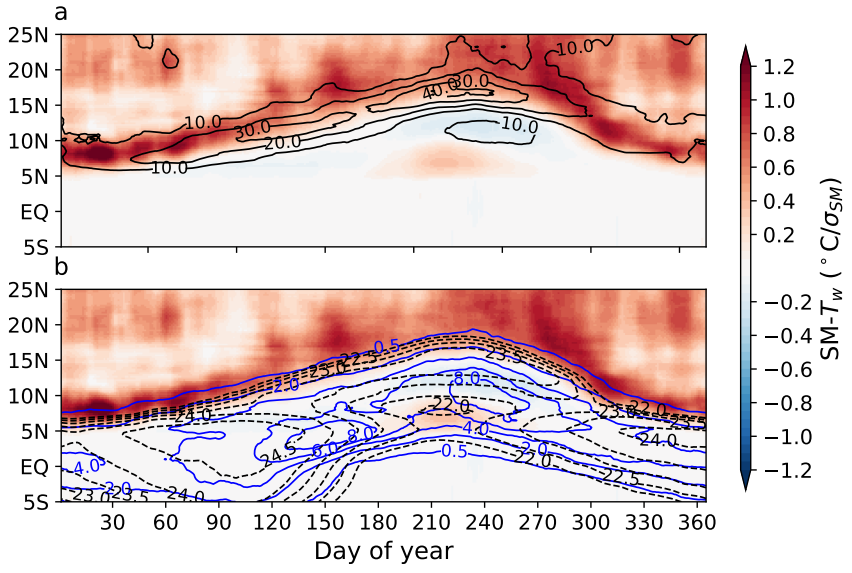

FIG. 4. Daily Sensitivity index I_{SM-T_w} zonally averaged over West Africa between 12° W and 6° E (shading in both (a) and (b)). Contours denote I_{SM-LH} $(W \cdot m^{-2}/\sigma_{SM})$ in (a) and daily precipitation (mm) (blue) and T_w (°C) (black) in (b). Both I_{SM-T_w} and I_{SM-LH} are calculated for each calendar day based on a surrounding 11-day window across 1950-2019. The seasonal cycle of T_w and precipitation are smoothed by taking a 11-day moving-average.

c. Diurnal variations in SM-T_w coupling

The diurnal cycle of SM-T_w coupling is also of interest since both daytime and nighttime heat stress are needed for evaluating heat accumulation within human body and may have different behaviors. Here we examine such diurnal variations in summer. Soil moisture is negatively correlated with T during both daytime and nighttime (Fig. S5), but this negative correlation is considerably weaker at night. This is possibly due to reduced surface longwave cooling under conditions with a more humid boundary layer conditional on wetter soil (Raymond et al. 2021). For I_{SM-T_w}, the daily mean pattern in figure 2d persists throughout the course of the day (Fig. 5). This is surprising since we hypothesized earlier that the distribution of SM-T_w coupling hotspots depends on soil moisture's control on the partitioning of incoming solar radiation between SH and LH. This obviously is a process only relevant in daytime. This diurnally consistent pattern therefore may result from a propagation of daytime signal to nighttime. Although broadly similar between daytime and nighttime, I_{SM-T_w} does show slight diurnal variations in terms of pattern and

Accepted for publication in *Journal of Climate*. DOI 10.1175/JCLI-D-23-0132.1.

magnitudes. For example, the eastern U.S. and southern South America to the east of the Andes show significantly positive I_{SM-T_w} during nighttime which is not found within daytime or in the daily mean (Fig. 5). Nighttime hours show slightly stronger positive and weaker negative I_{SM-T_w} compared with daytime (Fig. 5). These are probably due to reduced nighttime surface longwave cooling as soil moisture increases (Raymond et al. 2021). A significant positive coupling between soil moisture and T_w throughout the day (Fig. 5) suggests that both daytime and nighttime heat stress might be amplified under wet soil.

d. Local nonlinear structure in SM-T_w coupling

We assumed a linear relationship between soil moisture and T_w in calculating I_{SM-T_w} to simplify the interpretation of the results, but this approach has important limitations. T_w is not necessarily linearly related with soil moisture. Here we select one local area (characterized by a $2^\circ \times 2^\circ$ lat/lon box) within each SM-T_w coupling hotspot (Fig. 6) to examine the detailed structure of this relationship. The results are qualitatively similar among all local areas with the SM-T_w coupling hotspots. T_w varies non-linearly with soil moisture–it is characterized by an initial rapid increase of T_w with soil wetting which then plateaus or even decreases as soil moisture continues to increase (Fig. 7a). Thus, SM-T_w coupling is nonlinear with a dependence on the background SM levels. It can be much stronger within certain soil moisture range than that indicated by the linear sensitivity index across the whole range of soil moisture. For example, over the region within the Sahel zone (SAHL), T_w first rises by $\sim$1.3 °C/σ_{SM} under drier-than-normal soil which then plateaus generating a substantially lower I_{SM-T_w} of 1.0 °C/σ_{SM} across the whole range of soil moisture. $L_v q$ rises and $C_p T$ declines with increasing soil moisture. However, $L_v q$ increases more strongly and dominates the resultant variations in T_w. As discussed in Section 3a, the relatively muted changes of sensible heat compared with latent heat cannot be explained by the direct effect of energy re-partition which should result in equal and opposite changes in $C_p T$ and $L_v q$. Such asymmetry is possibly because a shallower PBL under wetter soil tends to mute the cooling and enlarge the moistening effect. The reduction of dry air entrainment may further amplify the latent heat increase (van Heerwaarden et al. 2009).

Such nonlinear SM-T_w relation may be associated with the covariations in soil moisture, solar radiation and ET. Incoming solar radiation consistently decreases with soil moisture (Fig. 7c).

Accepted for publication in *Journal of Climate*. DOI 10.1175/JCLI-D-23-0132.1.

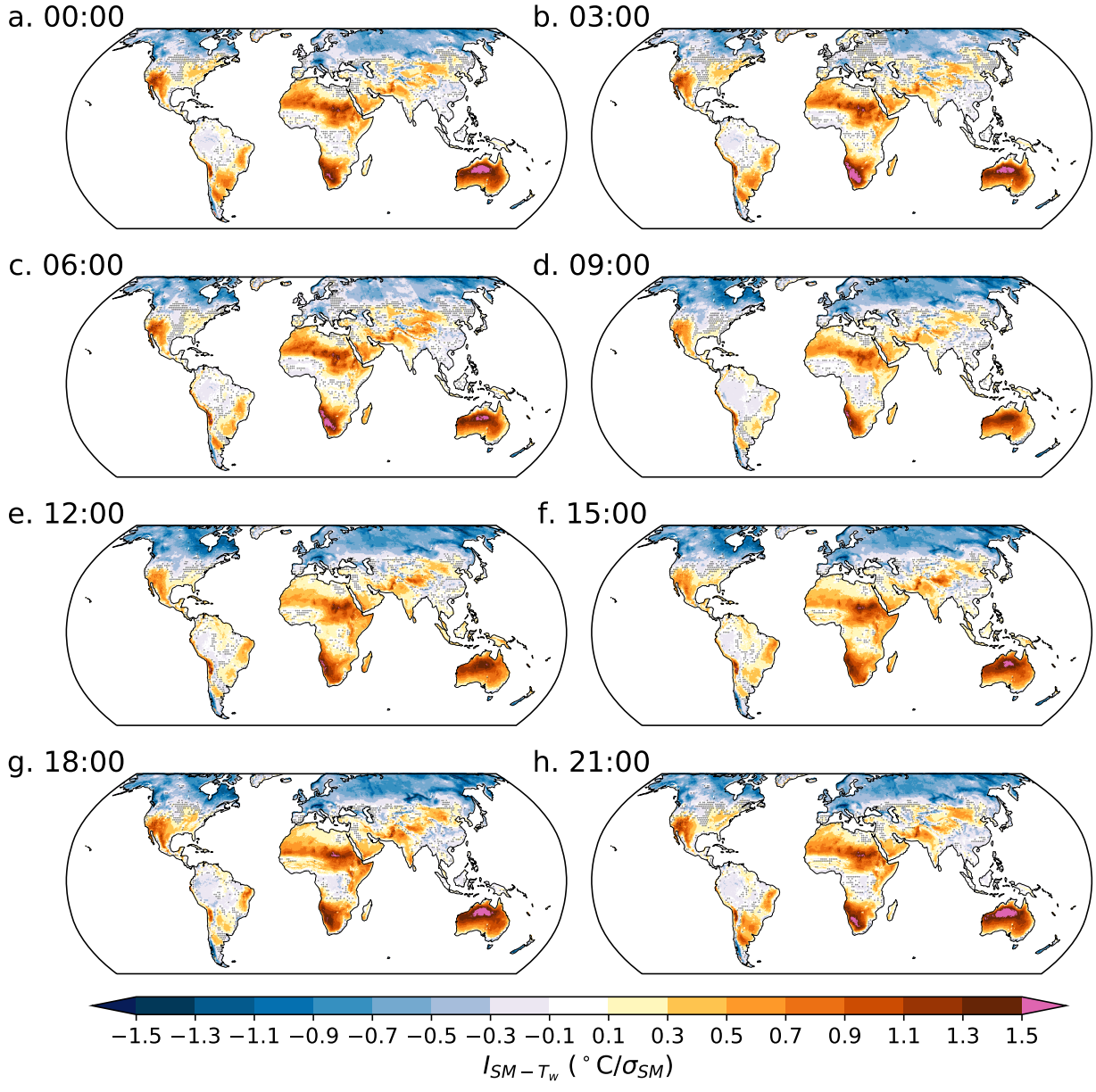

FIG. 5. Sub-daily (local time) sensitivity index I_{SM-T_w} during summer of 1950-2019. Stipples denote regions of statistical insignificance at 0.1% level.

This however is counteracted by changes in other radiation components at the beginning including a reduced surface longwave cooling, less reflected solar radiation, and more incoming long-wave radiation possibly due to increasing water vapor. As a result, net surface radiative energy remains stable initially or even slightly increases. This radiative energy at the surface is then spread into a shallower PBL under wetter soil which leads to the initial rapid increases of T_w. Afterwards,

Accepted for publication in *Journal of Climate*. DOI 10.1175/JCLI-D-23-0132.1.

declines in incoming solar radiation outpace changes in other radiation components causing a reduction of net radiative energy at surface with increasing soil moisture (Fig. 7c). This may contribute to the leveling off of T_w increases with soil moisture. Such covariations in soil moisture and solar radiation may also shift the region from transitional towards energy-limited ET regime. As a result, soil moisture variations cannot effectively control energy partition and PBL growth (Fig. 7d, e) which may also explain the plateau of T_w curves. The conclusions remain qualitatively unchanged when switching to other locations within each hotspot. However, averaging across a large region such as the entire hotspot smooths out the nonlinear structure leaving behind an approximately linear relationship.

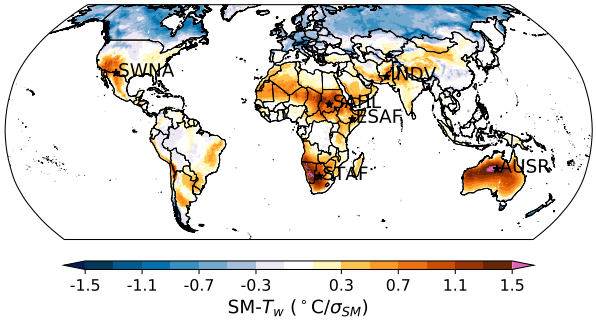

FIG. 6. Selected local regions within SM-T_w coupling hotspots including the one over southwest North America (SWNA: 30-32°N, 108-106°W), the Sahel zone (SAHL: 13-15°N, 28-30°E), East Africa (ESAF: 5-7°N, 42-44°E), South Africa (STAF: 26-24°S, 22-24°E), Australia (AUSR: 22-20°S, 133-135°E), and the Indus Valley (INDV: 28-30°N, 65-67°W). The background map shows I_{SM-T_w} during summer of 1950-2019.

e. Hot-days composite analysis

In previous sections, SM-T_w coupling is examined by calculating the coupling metric between daily average soil moisture and T_w from all days within the selected season. We identify regions with a positive relation between daily average soil moisture and T_w which is closely associated with soil moisture's control on surface energy partition. We want to know whether the coupling structure obtained from coupling metric analyses are robust to methodological choices on sampling strategy and statistical coupling quantification. Therefore, here we only sample hot-days (defined in methods) and compute the composite anomalies of soil moisture conditioned on hot-days from 1950 to 2019 (Fig. 8a). The spatial distribution of soil moisture anomalies from the hot-days composite

Accepted for publication in *Journal of Climate*. DOI 10.1175/JCLI-D-23-0132.1.

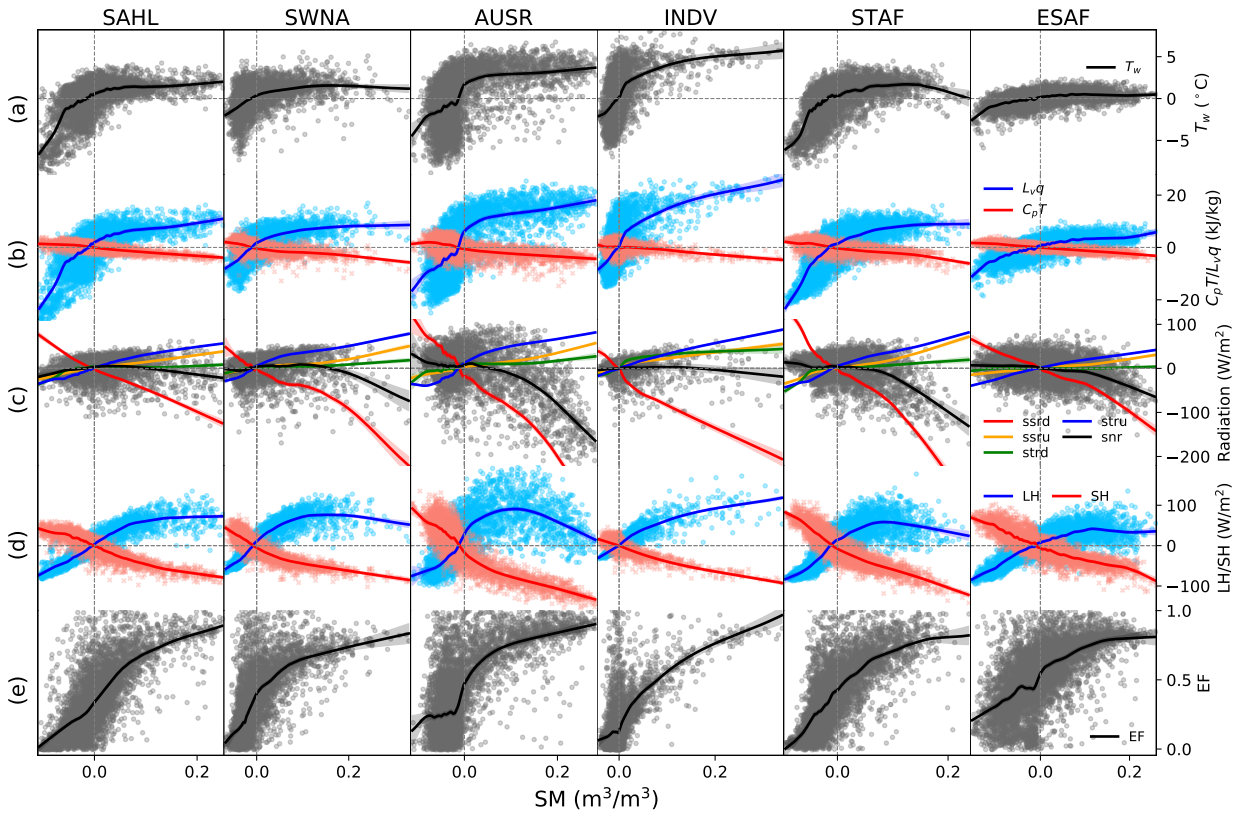

FIG. 7. Variations with soil moisture in (a) T_w, (b) C_pT and L_vq, (c) net radiative energy (snr), downward solar radiation (ssrd), surface reflected solar radiation (ssru), downward long-wave radiation (strd) and upwelling longwave radiation (stru) at surface, (d) LH and SH, and (e) evaporative fraction (EF) at six locations as shown in Fig. 6 during the summer of 1950-2019. The scatters in (c) represent snr. Anomalies are shown for whole-day average soil moisture, T_w, C_pT and L_vq, and daytime average surface turbulent and radiative fluxes; whereas absolute values are used for EF. Curves are generated through Generalized cross-validation (GCV)-optimized LOESS model fitting with the 95% confidence interval denoted by shading.

strongly resembles the pattern of I_{SM-T_w} (with a pattern correlation coefficient of 0.81 between Fig. 2d and Fig. 8a) suggesting that the SM-T_w coupling pattern is robust to methodological choices. We also calculate the composite anomalies in surface temperature, surface turbulent fluxes and PBLH, and examine their covariation with soil moisture anomalies. The SM-T_w coupling hotspots determined from coupling metric analyses consistently show wet soil anomalies (Fig. 8a) within the hot-days composite in combination with anomalously high LH (Fig. 8c) and low SH (Fig. 8d) from a cooler surface (Fig. 8b) and a shallower PBL (Fig. 8e). Such covariation in the

Accepted for publication in *Journal of Climate*. DOI 10.1175/JCLI-D-23-0132.1.

composite anomalies of soil moisture, surface heat fluxes and PBLH is consistent with the physical mechanism linking wetter soil to stronger heat stress as proposed by previous studies (Findell and Eltahir 2003a; Eltahir 1998; Pal and Eltahir 2001). Anomalously weak incoming solar radiation and weakly positive or even negative anomalies in Z500 are found over the SM-T_w coupling hotspots (Fig. 8f, g) indicating that hot-days in these regions are not driven by anomalously strong solar heating under the control of anticyclonic systems.

Outside of the SM-T_w coupling hotspots, the tropics and northern high latitudes show weakly wet or even dry soil moisture anomalies and anomalously strong incoming solar radiation (Fig. 8a, f) which are consistent with the energy-limited ET regime (Teuling et al. 2009; Seneviratne et al. 2010). Typical synoptic processes leading to hot T in middle and high latitudes such as blocking may also control some high T_w events (Ford and Schoof 2017; Raymond et al. 2017) indicated by the strong positive anomalies in Z500 (Fig. 8g). The interaction between high T values and dry soil (Fig. 8a) may further amplify these hot events.

T_w hot-days in several regions are characterized by anomalously wet soil which is in contrast to the widely-acknowledged amelioration of hot T under wet soil (Thiery et al. 2020, 2017; Kueppers et al. 2007). Since T_w reflects both T and q, such contrasting behavior of extremely high T_w and T values are expected to depend on the relative contributions of T and q anomalies to T_w exceedances on hot-days. If the T_w exceedances are mainly induced by anomalous hot T, we should expect similar behavior between extremely high T_w and T events. Therefore, here we show the relative contributions of T and q anomalies to T_w exceedances (Fig. 8k, l) which can help understand the coupling between soil moisture and T_w hot-days.

As described in the methods, T_w is a measure of moist enthalpy, and changes at the same rate in response to perturbations in C_pT and L_vq. Hence, we calculate composite anomalies in C_pT and L_vq to quantify the relative importance of sensible and latent heat anomalies in generating T_w hot-days (Fig. 8h, i). L_vq makes larger contributions to anomalous high T_w globally. The dominance of L_vq is especially remarkable in the SM-T_w coupling hotspots where C_pT is close to or even lower than the climatology average. This directly implies a lack of correlation between the dynamics of dry and humid heat waves in these regions.

Over northern high latitudes, C_pT and L_vq anomalies are of more comparable magnitudes which is consistent with the scenario of coherent changes in sensible and latent heat driven by variations

Accepted for publication in *Journal of Climate*. DOI 10.1175/JCLI-D-23-0132.1.

in incoming solar radiation. This suggests that in northern high latitudes moist heat stress behaves in a similar way as hot T events. This interpretation is supported by the fact that the T_w- and T-defined hot-days overlap with each other by more than 50% over that area (Fig. 1a). But they are nearly entirely separated (overlapping ratio<1%) from each other over some monsoon regions including the SM-T_w coupling hotspots.

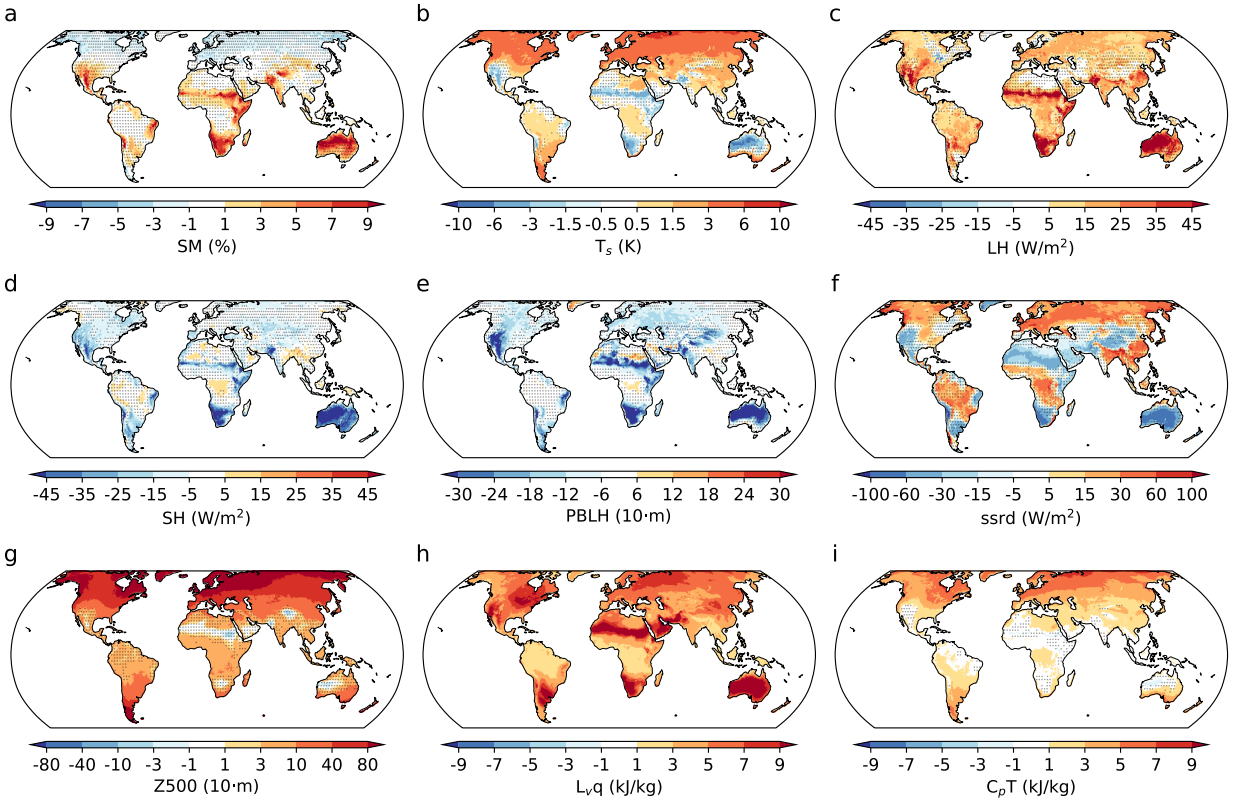

FIG. 8. Composite anomalies of (a) soil moisture, (b) T_s, (c) LH, (d) SH, (e) PBLH, (f) incoming solar radiation (ssrd), (g) Z500, (h) $L_v q$ and (i) $C_p T$ conditional on hot-days during 1950-2019. Anomalies are calculated for whole-day average soil moisture, Z500, $L_v q$ and $C_p T$ and daytime average T_s, LH, SH, PBLH and ssrd. Surface heat fluxes are positive upwards. Stipples indicate at least 2/3 of hot-days have anomalies of the same sign as the composite anomaly.

4. Discussion

A global picture of SM-T_w coupling and its seasonal and diurnal cycle have been derived from ERA5 reanalysis. In contrast to the well-established negative SM-T correlation, we found

Accepted for publication in *Journal of Climate*. DOI 10.1175/JCLI-D-23-0132.1.

widespread significant positive relationship between wetter soil and higher T_w values. The global SM-T_w coupling distribution agrees with previously reported results from localized studies. For example, significant positive SM-T_w coupling is found over climatologically wet areas of Indian subcontinent during pre- and post-monsoon seasons consistent with Guo et al. (2022) who found expanding irrigation to enhance pre- and post-monsoon T_w and wet-bulb globe temperature (WBGT) over urban areas of northern India. Monteiro and Caballero (2019) found that surface evaporation within the well-irrigated land flanking the Indus River plays a major role in generating extreme T_w values over the Indus Valley. Their findings are consistent with a significant positive SM-T_w coupling within that area (Fig. 2d). Speizer et al. (2022) found that extreme T_w values are far more likely than normal within days surrounding precipitation events in certain areas (Fig. 3e in their paper) the distribution of which well agrees with the SM-T_w coupling hotspots pattern. In Illinois, prior work found no significant correlation between soil moisture and T_w (Findell and Eltahir 1999), and oppressive heat waves (measured by equivalent temperature $T_e = (C_pT + L_vq)/C_p$) are triggered by anticyclonic features in the upper atmosphere in combination with surplus soil moisture from antecedent precipitation (Ford and Schoof 2017). We confirm these findings by showing weak SM-T_w coupling (Fig. 2d) and positive anomalies in Z500 (Fig. 8g) conditioned on T_w hot-days in Illinois. Nevertheless, our results demonstrate that the high-pressure anomalies are not transferable to the SM-T_w coupling hotspots where Z500 exhibits rather weak or even negative anomalies conditioned on T_w hot-days (Fig. 8g). We show that the SM-T_w coupling is nonlinear and can be especially strong within the dry range of soil moisture. This is consistent with prior work that found an increase in the sensitivity of T and surface heat fluxes to soil moisture variations as soil moisture progressively dries out and crosses a certain threshold (Dirmeyer et al. 2021; Benson and Dirmeyer 2021; Hsu and Dirmeyer 2022).

Regions with significant positive SM-T_w coupling belong to a transitional ET regime in which soil moisture effectively controls surface energy partition. The distribution of SM-T_w coupling hotspots also well agrees with that of land-atmosphere coupling hotspots revealed by previous studies (Schwingshackl et al. 2017; Koster 2004; Koster et al. 2006; Miralles et al. 2012; Dirmeyer 2011). This suggests that the positive SM-T_w coupling is to first order controlled by soil moisture's regulation of surface energy partition. Within SM-T_w coupling hotspots, high T_w days show wetter-than-normal soil, anomalous high LH and low SH from a cooler surface and a shallower PBL.

Accepted for publication in *Journal of Climate*. DOI 10.1175/JCLI-D-23-0132.1.

This is consistent with the previously proposed physical mechanism linking wetter soil to stronger heat stress–namely wet soil suppresses PBL growth and reduces free-troposphere air entrainment (Findell and Eltahir 2003a; Eltahir 1998; Pal and Eltahir 2001).

The tropics and high latitudes show negative SM-T_w consistent with an energy-limited ET regime (Teuling et al. 2009; Seneviratne et al. 2010). In addition, the chronically conditionally unstable troposphere over the tropics is sensitive to enhancement in PBL MSE which reduces the potential for the MSE to build-up within PBL (Zhang et al. 2021; Raymond et al. 2021; Williams and Renno 1993). The near moist adiabatic vertical profile over the tropics also makes T_w less responsive to the modulation of PBL growth and free-troposphere air entrainment. Furthermore, local extreme T_w in the tropics is under the nonlocal control of warmest SST elsewhere via tropical atmospheric dynamics (Buzan and Huber 2020; Zhang and Fueglistaler 2020; Zhang et al. 2021; Pierrehumbert 1995; Williams et al. 2009). All these factors contribute to a weak SM-T_w coupling in the tropics.

There are several limitations of this study. First, we use a linearly-formulated sensitivity index (Dirmeyer 2011) which may mask the essentially nonlinear structure of SM-T_w coupling. The SM-T_w coupling over certain soil moisture regimes could be much stronger than that indicated by the I_{SM-T_w} derived from the whole range of soil moisture. Climatologically wet regions could fall into transitional regime during droughts (Dirmeyer et al. 2021) and show positive SM-T_w coupling which however cannot be captured by a linear coupling metric across the whole sample. Nevertheless, the distribution of SM-T_w coupling hotspots as revealed in this study may still be robust since prior work found that superposing nonlinear components of SM-LE coupling does not alter the canonical land-atmospheric coupling distributions derived from linear coupling metrics (Hsu and Dirmeyer 2021, 2022). A related caveat is that soil moisture's control on surface energy partition within the transitional regime is hypothesized to be important for the occurrence of T_w hot days, but we did not demonstrate whether these hot days belong to transitional or energy-limited regime. Nonetheless, even if the evapotranspiration in most T_w hot days is energy-limited, the repartition of energy towards latent heat flux as soil getting wetter may still contribute to the build-up of high T_w values before reaching energy-limited regime. It must be acknowledged that soil moisture only represents one dimension of the physical control on extreme T_w values. Future work could investigate in more detail the nonlinear structure of the coupling between soil moisture and T_w. Techniques able to capture nonlinear relationship are required such as segmented

Accepted for publication in *Journal of Climate*. DOI 10.1175/JCLI-D-23-0132.1.

regression (Schwingshackl et al. 2017; Benson and Dirmeyer 2021; Dirmeyer et al. 2021; Hsu and Dirmeyer 2022) and machine learning (Zhao et al. 2019; Wang et al. 2022a). It is also of interest to investigate the distribution of T_w hot days across different soil moisture regimes which is useful in understanding the effects of surface energy repartition on enhancing T_w from high to extremely high values.

Second, soil moisture-heat stress coupling is expected to depend on the adopted heat stress metrics (Mishra et al. 2020) since different metrics weight humidity differently (Sherwood 2018; Buzan and Huber 2020). Compared with other commonly used heat stress metrics such as apparent temperature (Steadman 1984, 1994), heat index (Lans P. Rothfusz 1990; Steadman 1979), and WBGT (Yaglou and Minard 1957), T_w is heavily humidity-weighted (Sherwood 2018) which may favor a positive soil moisture-heat stress coupling. To provide a baseline for comparison, we calculate the coupling sensitivity index between soil moisture and heat index (Fig. S6) which places much less weight on humidity compared with T_w (Buzan et al. 2015). Heat index is generated using the National Weather Service adjusted formulation with the correction proposed by Romps and Lu (2022) to avoid bad heat index values at low temperatures. Negative correlation between soil moisture and heat index is found globally sharing a similar spatial pattern with I_{SM-T}. Among various heat stress metrics, WBGT represents a more comprehensive one containing the effects of not only temperature and humidity but also wind speed and radiation (Yaglou and Minard 1957). WBGT has a basis on both physiology and empirical calibration, and is considered a better representation of human physiological impacts of heat stress (Ioannou et al. 2022) being adopted by international (ISO 2017) and national occupational health guidelines (NIOSH 2016; ACGIH 2017). Compared with T_w, WBGT is less humidity-weighted and incorporates radiative heating. Hence, we expect the positive soil moisture-heat stress coupling to weaken or even become negative when replacing T_w with WBGT. Nonetheless, T_w constitutes 70% of WBGT (ignoring the difference between T_w and natural wet-bulb temperature) making our results potentially useful for WBGT-oriented applications as well. Future work could explicitly examine the coupling between soil moisture and WBGT as well as its individual components.

Finally, although we demonstrate an oft- positive correlation between soil moisture and T_w, this does not necessarily imply causality between wet soil and high T_w values. The correlation could result from covariations of soil moisture and T_w with other factors such as moisture transport.

Accepted for publication in *Journal of Climate*. DOI 10.1175/JCLI-D-23-0132.1.

For instance, the strong positive I_{SM-T_w} over Europe in winter (Fig. 3) is possibly due to an enhancement of both precipitation (and consequently soil moisture) and T_w via the transport of warm and humid marine air into the continent under the influence of the Gulf Stream.

More work is needed to establish causality between soil moisture and heat stress and understand the governing physics. It is valuable to compare both mean-level and extreme heat stress between irrigated and nearby non-irrigated areas that share similar synoptic forcing with a focus on comparing local surface fluxes and boundary layer dynamics (Rappin et al. 2021; Safieddine et al. 2022). The Granger causality test could also be used for determining whether prior soil moisture surplus is useful in predicting heat stress events (Granger 1969; Tuttle and Salvucci 2016). Model sensitivity experiments are essential in establishing causal attribution and disentangling the governing physical processes. Although the previously proposed physical mechanisms underlying positive SM-T_w coupling are readily justifiable under clear-sky condition (Findell and Eltahir 2003a; Wouters et al. 2022), once cloud forms above wet surface, the moisture ventilation from sub-cloud to cloud layer and cloud penetrative entrainment tend to warm and dry the mixed-layer which usually corresponds to a reduction in moist enthalpy (van Stratum et al. 2014). The blocking of incoming solar radiation may also reduce surface heat fluxes and T_w. It is unclear to what extent the cloud effects can counteract the clear-sky relation. The global distribution of SM-T_w coupling revealed in this study serves as a road map for such future studies which are especially warranted over regions/seasons with significant positive SM-T_w coupling.

5. Summary and implications

We examined the global distribution of SM-T_w coupling and its seasonal and diurnal cycle within ERA5 reanalysis. A significant positive relation between wetter soil and higher T_w values are found at several regions the distribution of which varies over the course of the year closely tied to monsoon development and corresponding changes in precipitation and soil moisture. We define the regions with significant positive SM-T_w coupling during local summer as SM-T_w coupling hotspots including Southwest North America, the Sahel zone, south and east Africa, the Indus Valley and Australia. The positive SM-T_w coupling is slightly stronger and more widespread during nighttime possibly due to reduced surface longwave cooling under conditions with a more humid boundary layer. Locally within the SM-T_w coupling hotspots, T_w varies nonlinearly with

Accepted for publication in *Journal of Climate*. DOI 10.1175/JCLI-D-23-0132.1.

soil moisture characterized by an initial rapid increase which then levels out or even decreases as soil moisture continues to increase. SM-T_w coupling hotspots are characterized by an effective control of soil moisture on surface energy partition, and well agree with the previously identified land-atmosphere coupling hotspots. High T_w days show anomalous wet soil, higher LH and lower SH from a cooler surface, and a shallower PBL. These are consistent with previously proposed physical mechanisms linking wet soil to stronger heat stress. The positive SM-T_w coupling suggests a possible amplification of heat stress when solar radiation is repartitioned from SH to LH.

Our results can potentially benefit heat stress prediction. It is important for climate models to capture the complex progression of SM-T_w covariation that we identified here in order to better predict heat stress. The I_{SM-T_w} distribution may serve as a target pattern for the validation of state-of-the-art climate models in CMIP6. Climate models have been demonstrated to have difficulty in accurately representing physical processes connecting soil, vegetation and energy partition (Swenson and Lawrence 2014; Tang and Riley 2013). The coupling between soil moisture and surface energy partition tends to be systematically overestimated, whereas the role of vegetation is underestimated (Williams et al. 2016; Ferguson et al. 2012). It is important for models to improve the representation of surface energy partition and boundary layer responses in order to better capture near-surface T, q and consequently heat stress. Given the long-memory of soil moisture (Orth and Seneviratne 2012; Seneviratne and Koster 2012), a good representation of soil moisture-heat stress coupling can improve the sub-seasonal to seasonal forecasting of heat stress (Koster et al. 2011; Seo et al. 2019).

This study also has broader implications on combating heat stress with land use and land managment strategies. Nature-based solutions have been increasingly adopted to mitigate urban heat island mainly in the form of 'greenspace' (e.g., green roof and facades, city parks, tree lined streets, etc.) and 'bluespace' (urban water bodies) (Zhou et al. 2023; Santamouris et al. 2017; Yu et al. 2020), such as the 'Million Tree Program' in many mega-cities (Frantzeskaki et al. 2019) and low-impact development with water-sensitive urban design (Coutts et al. 2014; He et al. 2019). These strategies reduce T mainly by increasing evapotranspiration although shading and heat storage changes also play a role (Oke et al. 1989; Rahman et al. 2015; Hu and Li 2020). However, our results question the effectiveness of evaporative cooling strategies in ameliorating moist heat stress. PBL growth may be suppressed with increasing fractions of vegetated or water

Accepted for publication in *Journal of Climate*. DOI 10.1175/JCLI-D-23-0132.1.

surfaces and reduced sensible heat flux (Sharma et al. 2016; Georgescu 2015) which may lead to a concentration of MSE within a shallower urban PBL and higher T_w values. In addition, vegetation such as green roof may slow down near-surface wind and reduce the wind cooling effect due to less downward momentum transport within a more stratified atmosphere (Sharma et al. 2016; Wang et al. 2022b). Therefore, we suggest reevaluating the effectiveness of evaporative cooling strategies in mitigating urban moist heat stress, and the results are expected to be sensitive to the regions and seasons under consideration (Hu and Li 2020). Such efforts are especially warranted given that the SM-T_w coupling hotspots cover several densely populated regions such as the West Africa and the Indus Valley. Globally, 42.0% of population are subject to significant (at 0.1% level) positive correlation between soil moisture and T_w in summer, and only 30.7% are faced with a significant negative correlation. In addition, the majority of the SM-T_w coupling hotspots identified here are less-developed regions and expected to experience fast urbanization in the coming decades.

Accepted for publication in *Journal of Climate*. DOI 10.1175/JCLI-D-23-0132.1.

Acknowledgments. This study is supported by NASA FINESST Grant 12000444; NSF 1805808-CBET Innovations at the Nexus of Food, Energy, and Water Systems (INFEWS: U.S.-China): A multiscale- integrated modeling approach to managing the transition to sustainability; NSF 1829764-OAC CyberTraining:CIU:Cross-disciplinary Training for Findable, Accessible, Interoperable, and Reusable (FAIR) science. The authors have no conflicts of interest or other ethical issues to disclose.

Data availability statement. ERA5 reanalysis data were downloaded from the Copernicus Climate Change Service (C3S) Climate Data Store (`https://cds.climate.copernicus.eu/cdsapp#!/dataset/reanalysis-era5-single-levels?tab=form`; `https://cds.climate.copernicus.eu/cdsapp#!/dataset/reanalysis-era5-single-levels-preliminary-back-extension?tab=form`). The results contain modified Copernicus Climate Change Service information 2020. Neither the European Commission nor ECMWF is responsible for any use that may be made of the Copernicus information or data it contains. Population data for the year 2020 was downloaded from `https://sedac.ciesin.columbia.edu/data/set/gpw-v4-population-count-adjusted-to-2015-unwpp-country-totals-rev11`.

APPENDIX

Sensitivity of wet bulb temperature to changes in sensible and latent heat

The isobaric T_w is defined as the solution of $T_w = T - L_v/C_p(q_w^* - q)$, where C_p is the specific heat of air at constant pressure; L_v is the latent heat of vaporization; q_w^* represents saturation specific humidity at temperature T_w. Based on this relation, it can be showed that

$$\frac{\partial T_w}{\partial (C_p T)} = \frac{1}{C_p + L_v \partial q_w^* / \partial T_w}. \tag{A1}$$

$$\frac{\partial T_w}{\partial (L_v q)} = \frac{1}{C_p + L_v \partial q_w^* / \partial T_w}. \tag{A2}$$

Therefore, the sensitivities of T_w to infinitesimally small perturbations in $C_p T$ and $L_v q$ are the same and depend on $\partial q_w^* / \partial T_w$. Through integration, T_w is also expected to change by the same amount in response to finite changes in $C_p T$ and $L_v q$ of the same magnitude.

Accepted for publication in *Journal of Climate*. DOI 10.1175/JCLI-D-23-0132.1.

References

ACGIH, 2017: 2017 tlvs and beis: Based on the documentation of the threshold limit values for chemical substances and physical agents and biological exposure indices. Tech. rep., ACGIH, Cincinnati.

Acosta, R. P., and M. Huber, 2020: Competing Topographic Mechanisms for the Summer Indo-Asian Monsoon. *Geophysical Research Letters*, **47 (3)**, https://doi.org/10.1029/2019GL085112.

Ambika, A. K., and V. Mishra, 2022: Improved Water Savings and Reduction in Moist Heat Stress Caused by Efficient Irrigation. *Earth's Future*, **10 (4)**, https://doi.org/10.1029/2021EF002642.

Aram, F., E. Higueras García, E. Solgi, and S. Mansournia, 2019: Urban green space cooling effect in cities. *Heliyon*, **5 (4)**, e01 339, https://doi.org/10.1016/j.heliyon.2019.e01339.

Balsamo, G., A. Beljaars, K. Scipal, P. Viterbo, B. van den Hurk, M. Hirschi, and A. K. Betts, 2009: A Revised Hydrology for the ECMWF Model: Verification from Field Site to Terrestrial Water Storage and Impact in the Integrated Forecast System. *Journal of Hydrometeorology*, **10 (3)**, 623–643, https://doi.org/10.1175/2008JHM1068.1.

Balsamo, G., and Coauthors, 2015: ERA-Interim/Land: a global land surface reanalysis data set. *Hydrology and Earth System Sciences*, **19 (1)**, 389–407, https://doi.org/10.5194/hess-19-389-2015.

Barriopedro, D., E. M. Fischer, J. Luterbacher, R. M. Trigo, and R. Garcia-Herrera, 2011: The Hot Summer of 2010: Redrawing the Temperature Record Map of Europe. *Science*, **332 (6026)**, 220–224, https://doi.org/10.1126/science.1201224.

Bell, B., and Coauthors, 2020: ERA5 hourly data on single levels from 1950 to 1978 (preliminary version). *Copernicus Climate Change Service (C3S) Climate Data Store (CDS)*, URL https://cds.climate.copernicus-climate.eu/cdsapp#!/dataset/reanalysis-era5-single-levels-preliminary-back-extension?tab=overview.

Benson, D. O., and P. A. Dirmeyer, 2021: Characterizing the Relationship between Temperature and Soil Moisture Extremes and Their Role in the Exacerbation of Heat Waves over the Contiguous United States. *Journal of Climate*, **34 (6)**, 2175–2187, https://doi.org/10.1175/JCLI-D-20-0440.1.

Accepted for publication in *Journal of Climate*. DOI 10.1175/JCLI-D-23-0132.1.

Betts, A. K., and J. H. Ball, 1995: The FIFE surface diurnal cycle climate. *Journal of Geophysical Research*, **100 (D12)**, 25 679, https://doi.org/10.1029/94JD03121.

Betts, A. K., and J. H. Ball, 1998: FIFE Surface Climate and Site-Average Dataset 1987–89. *Journal of the Atmospheric Sciences*, **55 (7)**, 1091–1108, https://doi.org/10.1175/1520-0469(1998)055⟨1091:FSCASA⟩2.0.CO;2.

Bohren, C., and B. Albrecht, 1998: *Atmospheric Thermodynamics*. Oxford University Press, New York.

Boussetta, S., G. Balsamo, A. Beljaars, T. Kral, and L. Jarlan, 2013: Impact of a satellite-derived leaf area index monthly climatology in a global numerical weather prediction model. *International Journal of Remote Sensing*, **34 (9-10)**, 3520–3542, https://doi.org/10.1080/01431161.2012.716543.

Brunner, L., N. Schaller, J. Anstey, J. Sillmann, and A. K. Steiner, 2018: Dependence of Present and Future European Temperature Extremes on the Location of Atmospheric Blocking. *Geophysical Research Letters*, https://doi.org/10.1029/2018GL077837.

Brunt, D., 1943: The reactions of the human body to its physical enviroment. *Quarterly Journal of the Royal Meteorological Society*, **69 (300)**, 77–114, https://doi.org/10.1002/qj.49706930002.

Buzan, J. R., and M. Huber, 2020: Moist Heat Stress on a Hotter Earth. *Annual Review of Earth and Planetary Sciences*, **48 (1)**, 623–655, https://doi.org/10.1146/annurev-earth-053018-060100.

Buzan, J. R., K. Oleson, and M. Huber, 2015: Implementation and comparison of a suite of heat stress metrics within the Community Land Model version 4.5. *Geoscientific Model Development*, **8 (2)**, 151–170, https://doi.org/10.5194/gmd-8-151-2015.

Center for International Earth Science Information Network - CIESIN - Columbia University, 2018: Gridded Population of the World, Version 4 (GPWv4): Population Count Adjusted to Match 2015 Revision of UN WPP Country Totals, Revision 11. NASA Socioeconomic Data and Applications Center (SEDAC), URL https://doi.org/10.7927/H4PN93PB, place: Palisades, NY.

Coffel, E. D., R. M. Horton, and A. de Sherbinin, 2018: Temperature and humidity based projections of a rapid rise in global heat stress exposure during the 21st century. *Environmental Research Letters*, **13 (1)**, 014 001, https://doi.org/10.1088/1748-9326/aaa00e.

Accepted for publication in *Journal of Climate*. DOI 10.1175/JCLI-D-23-0132.1.

Coffel, E. D., R. M. Horton, J. M. Winter, and J. S. Mankin, 2019: Nonlinear increases in extreme temperatures paradoxically dampen increases in extreme humid-heat. *Environmental Research Letters*, **14 (8)**, 084 003, https://doi.org/10.1088/1748-9326/ab28b7.

Cook, B. I., M. J. Puma, and N. Y. Krakauer, 2011: Irrigation induced surface cooling in the context of modern and increased greenhouse gas forcing. *Climate Dynamics*, **37 (7-8)**, 1587–1600, https://doi.org/10.1007/s00382-010-0932-x.

Coutts, A., M. Loughnan, N. Tapper, E. White, J. Thom, A. Broadbent, and R. Harris, 2014: The impacts of WSUD solutions on human thermal comfort: Green Cities and Micro-climate. Tech. rep., Cooperative Research Centre for Water Sensitive Cities, Melbourne, Australia.

Davies-Jones, R., 2008: An Efficient and Accurate Method for Computing the Wet-Bulb Temperature along Pseudoadiabats. *Monthly Weather Review*, **136 (7)**, 2764–2785, https://doi.org/10.1175/2007MWR2224.1.

de Freitas, C. R., and E. A. Grigorieva, 2015: A comprehensive catalogue and classification of human thermal climate indices. *International Journal of Biometeorology*, **59 (1)**, 109–120, https://doi.org/10.1007/s00484-014-0819-3.

de Rosnay, P., G. Balsamo, C. Albergel, J. Muñoz-Sabater, and L. Isaksen, 2014: Initialisation of Land Surface Variables for Numerical Weather Prediction. *Surveys in Geophysics*, **35 (3)**, 607–621, https://doi.org/10.1007/s10712-012-9207-x.

Diffenbaugh, N. S., and F. Giorgi, 2012: Climate change hotspots in the CMIP5 global climate model ensemble. *Climatic Change*, **114 (3-4)**, 813–822, https://doi.org/https://doi.org/10.1007/s10584-012-0570-x.

Dirmeyer, P. A., 2011: The terrestrial segment of soil moisture-climate coupling. *Geophysical Research Letters*, **38 (16)**, L16 702, https://doi.org/10.1029/2011GL048268.

Dirmeyer, P. A., G. Balsamo, E. M. Blyth, R. Morrison, and H. M. Cooper, 2021: Land-Atmosphere Interactions Exacerbated the Drought and Heatwave Over Northern Europe During Summer 2018. *AGU Advances*, **2 (2)**, https://doi.org/10.1029/2020AV000283.

Accepted for publication in *Journal of Climate*. DOI 10.1175/JCLI-D-23-0132.1.

Donat, M. G., A. J. Pitman, and S. I. Seneviratne, 2017: Regional warming of hot extremes accelerated by surface energy fluxes. *Geophysical Research Letters*, **44 (13)**, 7011–7019, https://doi.org/10.1002/2017GL073733.

Eltahir, E. A. B., 1998: A Soil Moisture-Rainfall Feedback Mechanism: 1. Theory and observations. *Water Resources Research*, **34 (4)**, 765–776, https://doi.org/10.1029/97WR03499.

Eltahir, E. A. B., and J. S. Pal, 1996: Relationship between surface conditions and subsequent rainfall in convective storms. *Journal of Geophysical Research: Atmospheres*, **101 (D21)**, 26 237–26 245, https://doi.org/10.1029/96JD01380.

Emanuel, K. A., 1995: On Thermally Direct Circulations in Moist Atmospheres. *Journal of the Atmospheric Sciences*, **52 (9)**, 1529–1534, https://doi.org/10.1175/1520-0469(1995)052⟨1529:OTDCIM⟩2.0.CO;2.

Ferguson, C. R., E. F. Wood, and R. K. Vinukollu, 2012: A Global Intercomparison of Modeled and Observed Land–Atmosphere Coupling. *Journal of Hydrometeorology*, **13 (3)**, 749–784, https://doi.org/10.1175/JHM-D-11-0119.1.

Fiala, D., and G. Havenith, 2015: Modelling Human Heat Transfer and Temperature Regulation. *The Mechanobiology and Mechanophysiology of Military-Related Injuries*, A. Gefen, and Y. Epstein, Eds., Vol. 19, Springer International Publishing, Cham, 265–302, https://doi.org/10.1007/8415_2015_183, URL http://link.springer.com/10.1007/8415_2015_183, series Title: Studies in Mechanobiology, Tissue Engineering and Biomaterials.

Findell, K. L., and E. A. B. Eltahir, 1999: Analysis of the pathways relating soil moisture and subsequent rainfall in Illinois. *Journal of Geophysical Research: Atmospheres*, **104 (D24)**, 31 565–31 574, https://doi.org/10.1029/1999JD900757.

Findell, K. L., and E. A. B. Eltahir, 2003a: Atmospheric Controls on Soil Moisture–Boundary Layer Interactions. Part I: Framework Development. *Journal of Hydrometeorology*, **4 (3)**, 552–569, https://doi.org/10.1175/1525-7541(2003)004⟨0552:ACOSML⟩2.0.CO;2.

Findell, K. L., and E. A. B. Eltahir, 2003b: Atmospheric Controls on Soil Moisture–Boundary Layer Interactions. Part II: Feedbacks within the Continental United States. *Journal of Hydrometeorology*, **4 (3)**, 570–583, https://doi.org/10.1175/1525-7541(2003)004⟨0570:ACOSML⟩2.0.CO;2.

Accepted for publication in *Journal of Climate*. DOI 10.1175/JCLI-D-23-0132.1.

Fischer, E. M., S. I. Seneviratne, P. L. Vidale, D. Lüthi, and C. Schär, 2007: Soil Moisture–Atmosphere Interactions during the 2003 European Summer Heat Wave. *Journal of Climate*, **20 (20)**, 5081–5099, https://doi.org/10.1175/JCLI4288.1.

Ford, T. W., and J. T. Schoof, 2017: Characterizing extreme and oppressive heat waves in Illinois. *Journal of Geophysical Research: Atmospheres*, **122 (2)**, 682–698, https://doi.org/10.1002/2016JD025721.

Foster, J., J. W. Smallcombe, S. Hodder, O. Jay, A. D. Flouris, L. Nybo, and G. Havenith, 2021: An advanced empirical model for quantifying the impact of heat and climate change on human physical work capacity. *International Journal of Biometeorology*, **65 (7)**, 1215–1229, https://doi.org/10.1007/s00484-021-02105-0.

Frantzeskaki, N., and Coauthors, 2019: Nature-Based Solutions for Urban Climate Change Adaptation: Linking Science, Policy, and Practice Communities for Evidence-Based Decision-Making. *BioScience*, **69 (6)**, 455–466, https://doi.org/10.1093/biosci/biz042.

Georgescu, M., 2015: Challenges Associated with Adaptation to Future Urban Expansion. *Journal of Climate*, **28 (7)**, 2544–2563, https://doi.org/10.1175/JCLI-D-14-00290.1.

Giles, J. A., C. G. Menéndez, and R. C. Ruscica, 2023: Nonlocal Impacts of Soil Moisture Variability in South America: Linking Two Land–Atmosphere Coupling Hot Spots. *Journal of Climate*, **36 (1)**, 227–242, https://doi.org/10.1175/JCLI-D-21-0510.1.

Granger, C. W. J., 1969: Investigating Causal Relations by Econometric Models and Cross-spectral Methods. *Econometrica*, **37 (3)**, 424, https://doi.org/10.2307/1912791.

Guo, Q., X. Zhou, Y. Satoh, and T. Oki, 2022: Irrigated cropland expansion exacerbates the urban moist heat stress in northern India. *Environmental Research Letters*, **17 (5)**, 054 013, https://doi.org/10.1088/1748-9326/ac64b6.

Haldane, J. S., 1905: The Influence of High Air Temperatures No. I. *Epidemiology and Infection*, **5 (4)**, 494–513, https://doi.org/10.1017/S0022172400006811.

Hauser, M., R. Orth, and S. I. Seneviratne, 2016: Role of soil moisture versus recent climate change for the 2010 heat wave in western russia. *Geophysical Research Letters*, **43 (6)**, 2819–2826, https://doi.org/https://doi.org/10.1002/2016GL068036.

Accepted for publication in *Journal of Climate*. DOI 10.1175/JCLI-D-23-0132.1.

He, B.-J., J. Zhu, D.-X. Zhao, Z.-H. Gou, J.-D. Qi, and J. Wang, 2019: Co-benefits approach: Opportunities for implementing sponge city and urban heat island mitigation. *Land Use Policy*, **86**, 147–157, https://doi.org/10.1016/j.landusepol.2019.05.003.

Hersbach, H., and Coauthors, 2020: The ERA5 global reanalysis. *Quarterly Journal of the Royal Meteorological Society*, **146 (730)**, 1999–2049, https://doi.org/10.1002/qj.3803.

Hsu, H., and P. A. Dirmeyer, 2021: Nonlinearity and Multivariate Dependencies in the Terrestrial Leg of Land-Atmosphere Coupling. *Water Resources Research*, **57 (2)**, https://doi.org/10.1029/2020WR028179.

Hsu, H., and P. A. Dirmeyer, 2022: Deconstructing the soil moisture-latent heat flux relationship: the range of coupling regimes experienced and the presence of nonlinearity within the sensitive regime. *Journal of Hydrometeorology*, https://doi.org/10.1175/JHM-D-21-0224.1.

Hu, L., and Q. Li, 2020: Greenspace, bluespace, and their interactive influence on urban thermal environments. *Environmental Research Letters*, **15 (3)**, 034 041, https://doi.org/10.1088/1748-9326/ab6c30.

Im, E.-S., J. S. Pal, and E. A. B. Eltahir, 2017: Deadly heat waves projected in the densely populated agricultural regions of South Asia. *Science Advances*, **3 (8)**, e1603 322, https://doi.org/10.1126/sciadv.1603322.

Ioannou, L. G., and Coauthors, 2022: Indicators to assess physiological heat strain – Part 3: Multi-country field evaluation and consensus recommendations. *Temperature*, **9 (3)**, 274–291, https://doi.org/10.1080/23328940.2022.2044739.

ISO, 2017: Ergonomics of the thermal environment — Assessment of heat stress using the WBGT (wet bulb globe temperature) index. International Standard, International Organization for Standardization (ISO), Geneva.

Ivanovich, C., W. Anderson, R. Horton, C. Raymond, and A. Sobel, 2022: The Influence of Intraseasonal Oscillations on Humid Heat in the Persian Gulf and South Asia. *Journal of Climate*, 1–48, https://doi.org/10.1175/JCLI-D-21-0488.1.

Accepted for publication in *Journal of Climate*. DOI 10.1175/JCLI-D-23-0132.1.

Jha, R., A. Mondal, A. Devanand, M. K. Roxy, and S. Ghosh, 2022: Limited influence of irrigation on pre-monsoon heat stress in the Indo-Gangetic Plain. *Nature Communications*, **13 (1)**, 4275, https://doi.org/10.1038/s41467-022-31962-5.

Kang, S., and E. A. B. Eltahir, 2018: North China Plain threatened by deadly heatwaves due to climate change and irrigation. *Nature Communications*, **9 (1)**, 2894, https://doi.org/10.1038/s41467-018-05252-y.

Kiladis, G. N., and H. F. Diaz, 1989: Global Climatic Anomalies Associated with Extremes in the Southern Oscillation. *Journal of Climate*, **2 (9)**, 1069–1090, https://doi.org/10.1175/1520-0442(1989)002⟨1069:GCAAWE⟩2.0.CO;2.

Kong, Q., and M. Huber, 2022: Explicit calculations of Wet Bulb Globe Temperature compared with approximations and why it matters for labor productivity. *Earth's Future*, https://doi.org/10.1029/2021EF002334.

Koster, R. D., 2004: Regions of Strong Coupling Between Soil Moisture and Precipitation. *Science*, **305 (5687)**, 1138–1140, https://doi.org/10.1126/science.1100217.

Koster, R. D., and Coauthors, 2006: GLACE: The Global Land–Atmosphere Coupling Experiment. Part I: Overview. *Journal of Hydrometeorology*, **7 (4)**, 590–610, https://doi.org/10.1175/JHM510.1.

Koster, R. D., and Coauthors, 2011: The Second Phase of the Global Land–Atmosphere Coupling Experiment: Soil Moisture Contributions to Subseasonal Forecast Skill. *Journal of Hydrometeorology*, **12 (5)**, 805–822, https://doi.org/10.1175/2011JHM1365.1, URL http://journals.ametsoc.org/doi/10.1175/2011JHM1365.1.

Krakauer, N. Y., B. I. Cook, and M. J. Puma, 2020: Effect of irrigation on humid heat extremes. *Environmental Research Letters*, **15 (9)**, 094 010, https://doi.org/10.1088/1748-9326/ab9ecf.

Krayenhoff, E. S., M. Moustaoui, A. M. Broadbent, V. Gupta, and M. Georgescu, 2018: Diurnal interaction between urban expansion, climate change and adaptation in US cities. *Nature Climate Change*, **8 (12)**, 1097–1103, https://doi.org/10.1038/s41558-018-0320-9.

Accepted for publication in *Journal of Climate*. DOI 10.1175/JCLI-D-23-0132.1.

Kueppers, L. M., M. A. Snyder, and L. C. Sloan, 2007: Irrigation cooling effect: Regional climate forcing by land-use change. *Geophysical Research Letters*, **34 (3)**, L03 703, https://doi.org/10.1029/2006GL028679.

Lans P. Rothfusz, 1990: The heat index equation (or, more than you ever wanted to know about heat index). Tech. Rep. SR 90-23, National Oceanic and Atmospheric Administration, National Weather Service, Office of Meteorology, Fort Worth, Texas.

Lehnert, M., V. Tokar, M. Jurek, and J. Geletič, 2021: Summer thermal comfort in Czech cities: measured effects of blue and green features in city centres. *International Journal of Biometeorology*, **65 (8)**, 1277–1289, https://doi.org/10.1007/s00484-020-02010-y.

Lejeune, Q., S. I. Seneviratne, and E. L. Davin, 2017: Historical Land-Cover Change Impacts on Climate: Comparative Assessment of LUCID and CMIP5 Multimodel Experiments. *Journal of Climate*, **30 (4)**, 1439–1459, https://doi.org/10.1175/JCLI-D-16-0213.1.

Li, D., J. Yuan, and R. E. Kopp, 2020a: Escalating global exposure to compound heat-humidity extremes with warming. *Environmental Research Letters*, **15 (6)**, 064 003, https://doi.org/10.1088/1748-9326/ab7d04.

Li, K., J. Zhang, L. Wu, K. Yang, and S. Li, 2022: The Role of Soil Temperature Feedbacks for Summer Air Temperature Variability Under Climate Change Over East Asia. *Earth's Future*, **10 (4)**, https://doi.org/10.1029/2021EF002377.

Li, M., P. Wu, and Z. Ma, 2020b: A comprehensive evaluation of soil moisture and soil temperature from third-generation atmospheric and land reanalysis data sets. *International Journal of Climatology*, **40 (13)**, 5744–5766, https://doi.org/10.1002/joc.6549.

Lobell, D. B., C. Bonfils, and J.-M. Faurès, 2008: The Role of Irrigation Expansion in Past and Future Temperature Trends. *Earth Interactions*, **12 (3)**, 1–11, https://doi.org/10.1175/2007EI241.1.

Luo, M., and N.-C. Lau, 2019: Amplifying effect of ENSO on heat waves in China. *Climate Dynamics*, **52 (5-6)**, 3277–3289, https://doi.org/10.1007/s00382-018-4322-0.

Accepted for publication in *Journal of Climate*. DOI 10.1175/JCLI-D-23-0132.1.

Mahto, S. S., and V. Mishra, 2019: Does ERA-5 Outperform Other Reanalysis Products for Hydrologic Applications in India? *Journal of Geophysical Research: Atmospheres*, **124 (16)**, 9423–9441, https://doi.org/10.1029/2019JD031155.

Matthews, T., M. Byrne, R. Horton, C. Murphy, R. Pielke, C. Raymond, P. Thorne, and R. L. Wilby, 2022: Latent heat must be visible in climate communications. *WIREs Climate Change*, https://doi.org/10.1002/wcc.779.

Miralles, D. G., A. J. Teuling, C. C. van Heerwaarden, and J. Vilà-Guerau de Arellano, 2014: Mega-heatwave temperatures due to combined soil desiccation and atmospheric heat accumulation. *Nature Geoscience*, **7 (5)**, 345–349, https://doi.org/10.1038/ngeo2141.

Miralles, D. G., M. J. van den Berg, A. J. Teuling, and R. A. M. de Jeu, 2012: Soil moisture-temperature coupling: A multiscale observational analysis: soil moisture-temperature coupling. *Geophysical Research Letters*, **39 (21)**, n/a–n/a, https://doi.org/10.1029/2012GL053703.

Mishra, V., A. K. Ambika, A. Asoka, S. Aadhar, J. Buzan, R. Kumar, and M. Huber, 2020: Moist heat stress extremes in India enhanced by irrigation. *Nature Geoscience*, **13 (11)**, 722–728, https://doi.org/10.1038/s41561-020-00650-8.

Monteiro, J. M., and R. Caballero, 2019: Characterization of Extreme Wet-Bulb Temperature Events in Southern Pakistan. *Geophysical Research Letters*, **46 (17-18)**, 10 659–10 668, https://doi.org/10.1029/2019GL084711.

Neal, E., C. S. Y. Huang, and N. Nakamura, 2022: The 2021 Pacific Northwest Heat Wave and Associated Blocking: Meteorology and the Role of an Upstream Cyclone as a Diabatic Source of Wave Activity. *Geophysical Research Letters*, **49 (8)**, https://doi.org/10.1029/2021GL097699.

Nie, J., W. R. Boos, and Z. Kuang, 2010: Observational Evaluation of a Convective Quasi-Equilibrium View of Monsoons. *Journal of Climate*, **23 (16)**, 4416–4428, https://doi.org/10.1175/2010JCLI3505.1.

NIOSH, 2016: Criteria for a Recommended Standard: Occupational Exposure to Heat and Hot Environments. Tech. Rep. DHHS (NIOSH) Publication No. 2016-106, DHHS, NIOSH, Washington, D.C.

Accepted for publication in *Journal of Climate*. DOI 10.1175/JCLI-D-23-0132.1.

Oke, T. R., and Coauthors, 1989: The micrometeorology of the urban forest. *Philosophical Transactions of the Royal Society of London. B, Biological Sciences*, **324 (1223)**, 335–349, https://doi.org/10.1098/rstb.1989.0051.

Orth, R., and S. I. Seneviratne, 2012: Analysis of soil moisture memory from observations in Europe. *Journal of Geophysical Research: Atmospheres*, **117**, D15 115, https://doi.org/10.1029/2011JD017366.

Pal, J. S., and E. A. B. Eltahir, 2001: Pathways Relating Soil Moisture Conditions to Future Summer Rainfall within a Model of the Land–Atmosphere System. *Journal of Climate*, **14 (6)**, 1227–1242, https://doi.org/10.1175/1520-0442(2001)014⟨1227:PRSMCT⟩2.0.CO;2.

Pal, J. S., and E. A. B. Eltahir, 2016: Future temperature in southwest Asia projected to exceed a threshold for human adaptability. *Nature Climate Change*, **6 (2)**, 197–200, https://doi.org/10.1038/nclimate2833.

Parker, T. J., G. J. Berry, M. J. Reeder, and N. Nicholls, 2014: Modes of climate variability and heat waves in Victoria, southeastern Australia. *Geophysical Research Letters*, **41 (19)**, 6926–6934, https://doi.org/10.1002/2014GL061736.

Pierrehumbert, R. T., 1995: Thermostats, Radiator Fins, and the Local Runaway Greenhouse. *Journal of the Atmospheric Sciences*, **52 (10)**, 1784–1806, https://doi.org/10.1175/1520-0469(1995)052⟨1784:TRFATL⟩2.0.CO;2.

Pozo-Vázquez, D., S. R. Gámiz-Fortis, J. Tovar-Pescador, M. J. Esteban-Parra, and Y. Castro-Díez, 2005: El Niño-southern oscillation events and associated European winter precipitation anomalies. *International Journal of Climatology*, **25 (1)**, 17–31, https://doi.org/10.1002/joc.1097.

Rahman, M. A., D. Armson, and A. R. Ennos, 2015: A comparison of the growth and cooling effectiveness of five commonly planted urban tree species. *Urban Ecosystems*, **18 (2)**, 371–389, https://doi.org/10.1007/s11252-014-0407-7, URL http://link.springer.com/10.1007/s11252-014-0407-7.

Accepted for publication in *Journal of Climate*. DOI 10.1175/JCLI-D-23-0132.1.

Rappin, E., and Coauthors, 2021: The Great Plains Irrigation Experiment (GRAINEX). *Bulletin of the American Meteorological Society*, **102 (9)**, E1756–E1785, https://doi.org/10.1175/BAMS-D-20-0041.1.

Raymond, C., T. Matthews, and R. M. Horton, 2020: The emergence of heat and humidity too severe for human tolerance. *Science Advances*, **6 (19)**, eaaw1838, https://doi.org/10.1126/sciadv.aaw1838.

Raymond, C., T. Matthews, R. M. Horton, E. M. Fischer, S. Fueglistaler, C. Ivanovich, L. Suarez-Gutierrez, and Y. Zhang, 2021: On the Controlling Factors for Globally Extreme Humid Heat. *Geophysical Research Letters*, **48 (23)**, https://doi.org/10.1029/2021GL096082.

Raymond, C., D. Singh, and R. M. Horton, 2017: Spatiotemporal Patterns and Synoptics of Extreme Wet-Bulb Temperature in the Contiguous United States. *Journal of Geophysical Research-Atmospheres*, **122 (24)**, 13 108–13 124, https://doi.org/10.1002/2017JD027140.

Romps, D. M., and Y.-C. Lu, 2022: Chronically underestimated: a reassessment of US heat waves using the extended heat index. *Environmental Research Letters*, **17 (9)**, 094 017, https://doi.org/10.1088/1748-9326/ac8945.

Saeed, W., I. Haqiqi, Q. Kong, M. Huber, J. R. Buzan, S. Chonabayashi, K. Motohashi, and T. W. Hertel, 2022: The Poverty Impacts of Labor Heat Stress in West Africa Under a Warming Climate. *Earth's Future*, **10 (11)**, https://doi.org/10.1029/2022EF002777.

Safieddine, S., C. Clerbaux, L. Clarisse, S. Whitburn, and E. A. B. Eltahir, 2022: Present and future land surface and wet bulb temperatures in the Arabian Peninsula. *Environmental Research Letters*, **17 (4)**, 044 029, https://doi.org/10.1088/1748-9326/ac507c.

Santamouris, M., L. Ding, F. Fiorito, P. Oldfield, P. Osmond, R. Paolini, D. Prasad, and A. Synnefa, 2017: Passive and active cooling for the outdoor built environment – Analysis and assessment of the cooling potential of mitigation technologies using performance data from 220 large scale projects. *Solar Energy*, **154**, 14–33, https://doi.org/10.1016/j.solener.2016.12.006.

Schwingshackl, C., M. Hirschi, and S. I. Seneviratne, 2017: Quantifying Spatiotemporal Variations of Soil Moisture Control on Surface Energy Balance and Near-Surface Air Temperature. *Journal of Climate*, **30 (18)**, 7105–7124, https://doi.org/10.1175/JCLI-D-16-0727.1.

Accepted for publication in *Journal of Climate*. DOI 10.1175/JCLI-D-23-0132.1.

Schär, C., D. Lüthi, U. Beyerle, and E. Heise, 1999: The Soil–Precipitation Feedback: A Process Study with a Regional Climate Model. *Journal of Climate*, **12 (3)**, 722–741, https://doi.org/10.1175/1520-0442(1999)012⟨0722:TSPFAP⟩2.0.CO;2.

Seneviratne, S. I., T. Corti, E. L. Davin, M. Hirschi, E. B. Jaeger, I. Lehner, B. Orlowsky, and A. J. Teuling, 2010: Investigating soil moisture–climate interactions in a changing climate: A review. *Earth-Science Reviews*, **99 (3-4)**, 125–161, https://doi.org/10.1016/j.earscirev.2010.02.004.

Seneviratne, S. I., and R. D. Koster, 2012: A Revised Framework for Analyzing Soil Moisture Memory in Climate Data: Derivation and Interpretation. *Journal of Hydrometeorology*, **13 (1)**, 404–412, https://doi.org/10.1175/JHM-D-11-044.1, URL http://journals.ametsoc.org/doi/10.1175/JHM-D-11-044.1.

Seneviratne, S. I., D. Lüthi, M. Litschi, and C. Schär, 2006: Land–atmosphere coupling and climate change in Europe. *Nature*, **443 (7108)**, 205–209, https://doi.org/10.1038/nature05095.

Seo, E., and Coauthors, 2019: Impact of soil moisture initialization on boreal summer subseasonal forecasts: mid-latitude surface air temperature and heat wave events. *Climate Dynamics*, **52 (3-4)**, 1695–1709, https://doi.org/10.1007/s00382-018-4221-4, URL http://link.springer.com/10.1007/s00382-018-4221-4.

Sharma, A., P. Conry, H. J. S. Fernando, A. F. Hamlet, J. J. Hellmann, and F. Chen, 2016: Green and cool roofs to mitigate urban heat island effects in the Chicago metropolitan area: evaluation with a regional climate model. *Environmental Research Letters*, **11 (6)**, 064 004, https://doi.org/10.1088/1748-9326/11/6/064004.

Shekhar, R., and W. R. Boos, 2017: Weakening and Shifting of the Saharan Shallow Meridional Circulation during Wet Years of the West African Monsoon. *Journal of Climate*, **30 (18)**, 7399–7422, https://doi.org/10.1175/JCLI-D-16-0696.1.

Sherwood, S. C., 2018: How Important Is Humidity in Heat Stress? *Journal of Geophysical Research-Atmospheres*, **123 (21)**, 11 808–11 810, https://doi.org/10.1029/2018JD028969.

Sherwood, S. C., and M. Huber, 2010: An adaptability limit to climate change due to heat stress. *Proceedings of the National Academy of Sciences*, **107 (21)**, 9552–9555, https://doi.org/10.1073/pnas.0913352107.

Accepted for publication in *Journal of Climate*. DOI 10.1175/JCLI-D-23-0132.1.

Song, F., G. J. Zhang, V. Ramanathan, and L. R. Leung, 2022: Trends in surface equivalent potential temperature: A more comprehensive metric for global warming and weather extremes. *Proceedings of the National Academy of Sciences*, **119 (6)**, e2117832 119, https://doi.org/10.1073/pnas.2117832119.

Speizer, S., C. Raymond, C. Ivanovich, and R. M. Horton, 2022: Concentrated and Intensifying Humid Heat Extremes in the IPCC AR6 Regions. *Geophysical Research Letters*, **49 (5)**, https://doi.org/10.1029/2021GL097261.

Steadman, R. G., 1979: The Assessment of Sultriness. Part I: A Temperature-Humidity Index Based on Human Physiology and Clothing Science. *Journal of Applied Meteorology*, **18 (7)**, 861–873, https://doi.org/10.1175/1520-0450(1979)018⟨0861:TAOSPI⟩2.0.CO;2.

Steadman, R. G., 1984: A Universal Scale of Apparent Temperature. *Journal of Climate and Applied Meteorology*, **23 (12)**, 1674–1687, https://doi.org/10.1175/1520-0450(1984)023⟨1674:AUSOAT⟩2.0.CO;2.

Steadman, R. G., 1994: Norms of apparent temperature in australia. *Aust. Met. Mag*, **43**, 1–16.

Swenson, S. C., and D. M. Lawrence, 2014: Assessing a dry surface layer-based soil resistance parameterization for the Community Land Model using GRACE and FLUXNET-MTE data. *Journal of Geophysical Research: Atmospheres*, **119 (17)**, 10,299–10,312, https://doi.org/10.1002/2014JD022314.

Tang, J., and W. J. Riley, 2013: Impacts of a new bare-soil evaporation formulation on site, regional, and global surface energy and water budgets in CLM4. *Journal of Advances in Modeling Earth Systems*, **5 (3)**, 558–571, https://doi.org/10.1002/jame.20034.

Teuling, A. J., and Coauthors, 2009: A regional perspective on trends in continental evaporation. *Geophysical Research Letters*, **36 (2)**, L02 404, https://doi.org/10.1029/2008GL036584.

Thiery, W., E. L. Davin, D. M. Lawrence, A. L. Hirsch, M. Hauser, and S. I. Seneviratne, 2017: Present-day irrigation mitigates heat extremes. *Journal of Geophysical Research: Atmospheres*, **122 (3)**, 1403–1422, https://doi.org/10.1002/2016JD025740.

Thiery, W., and Coauthors, 2020: Warming of hot extremes alleviated by expanding irrigation. *Nature Communications*, **11 (1)**, 290, https://doi.org/10.1038/s41467-019-14075-4.

Accepted for publication in *Journal of Climate*. DOI 10.1175/JCLI-D-23-0132.1.

Tuttle, S., and G. Salvucci, 2016: Empirical evidence of contrasting soil moisture–precipitation feedbacks across the United States. *Science*, **352 (6287)**, 825–828, https://doi.org/10.1126/science.aaa7185.

van Heerwaarden, C. C., J. Vilà-Guerau de Arellano, A. F. Moene, and A. A. M. Holtslag, 2009: Interactions between dry-air entrainment, surface evaporation and convective boundary-layer development. *Quarterly Journal of the Royal Meteorological Society*, **135 (642)**, 1277–1291, https://doi.org/10.1002/qj.431.

van Stratum, B. J. H., J. Vilá-Guerau de Arellano, C. C. van Heerwaarden, and H. G. Ouwersloot, 2014: Subcloud-Layer Feedbacks Driven by the Mass Flux of Shallow Cumulus Convection over Land. *Journal of the Atmospheric Sciences*, **71 (3)**, 881–895, https://doi.org/10.1175/JAS-D-13-0192.1.

Vecellio, D. J., S. T. Wolf, R. M. Cottle, and W. L. Kenney, 2022: Evaluating the 35°C wet-bulb temperature adaptability threshold for young, healthy subjects (PSU HEAT Project). *Journal of Applied Physiology*, **132 (2)**, 340–345, https://doi.org/10.1152/japplphysiol.00738.2021.

Virtanen, P., and Coauthors, 2020: SciPy 1.0: Fundamental Algorithms for Scientific Computing in Python. *Nature Methods*, **17**, 261–272, https://doi.org/10.1038/s41592-019-0686-2.

Vogel, M. M., R. Orth, F. Cheruy, S. Hagemann, R. Lorenz, B. J. J. M. Hurk, and S. I. Seneviratne, 2017: Regional amplification of projected changes in extreme temperatures strongly controlled by soil moisture-temperature feedbacks. *Geophysical Research Letters*, **44 (3)**, 1511–1519, https://doi.org/10.1002/2016GL071235.

Völker, S., H. Baumeister, T. Claßen, C. Hornberg, and T. Kistemann, 2013: Evidence for the temperature-mitigating capacity of urban blue space – a health geographic perspective. *Erdkunde*, **67 (04)**, 355–371, https://doi.org/10.3112/erdkunde.2013.04.05.

Wang, R., and Coauthors, 2022a: Recent increase in the observation-derived land evapotranspiration due to global warming. *Environmental Research Letters*, **17 (2)**, 024 020, https://doi.org/10.1088/1748-9326/ac4291.

Accepted for publication in *Journal of Climate*. DOI 10.1175/JCLI-D-23-0132.1.

Wang, X., H. Li, and S. Sodoudi, 2022b: The effectiveness of cool and green roofs in mitigating urban heat island and improving human thermal comfort. *Building and Environment*, 109082, https://doi.org/10.1016/j.buildenv.2022.109082.

Wei, J., and P. A. Dirmeyer, 2012: Dissecting soil moisture-precipitation coupling. *Geophysical Research Letters*, **39 (19)**, n/a–n/a, https://doi.org/10.1029/2012GL053038.

Willett, K. M., and S. Sherwood, 2010: Exceedance of heat index thresholds for 15 regions under a warming climate using the wet-bulb globe temperature. *International journal of climatology*, **32 (2)**, 161–177, https://doi.org/10.1002/joc.2257.

Williams, E., and N. Renno, 1993: An Analysis of the Conditional Instability of the Tropical Atmosphere. *Monthly Weather Review*, **121 (1)**, 21–36, https://doi.org/10.1175/1520-0493(1993)121⟨0021:AAOTCI⟩2.0.CO;2.

Williams, I. N., Y. Lu, L. M. Kueppers, W. J. Riley, S. C. Biraud, J. E. Bagley, and M. S. Torn, 2016: Land-atmosphere coupling and climate prediction over the U.S. Southern Great Plains. *Journal of Geophysical Research: Atmospheres*, **121 (20)**, https://doi.org/10.1002/2016JD025223.

Williams, I. N., R. T. Pierrehumbert, and M. Huber, 2009: Global warming, convective threshold and false thermostats. *Geophysical Research Letters*, **36 (21)**, L21 805, https://doi.org/10.1029/2009GL039849.

Wouters, H., J. Keune, I. Y. Petrova, C. C. van Heerwaarden, A. J. Teuling, J. S. Pal, J. Vilà-Guerau de Arellano, and D. G. Miralles, 2022: Soil drought can mitigate deadly heat stress thanks to a reduction of air humidity. *Science Advances*, **8 (1)**, eabe6653, https://doi.org/10.1126/sciadv.abe6653.

Xu, Z., R. Mahmood, Z. Yang, C. Fu, and H. Su, 2015: Investigating diurnal and seasonal climatic response to land use and land cover change over monsoon Asia with the Community Earth System Model. *Journal of Geophysical Research: Atmospheres*, **120 (3)**, 1137–1152, https://doi.org/10.1002/2014JD022479.

Yaglou, C. P., and D. Minard, 1957: Control of heat casualties at military training centers. *A.M.A. archives of industrial health*, **16 (4)**, 302–316.

Accepted for publication in *Journal of Climate*. DOI 10.1175/JCLI-D-23-0132.1.

Yang, S., J. Zeng, W. Fan, and Y. Cui, 2022: Evaluating Root-Zone Soil Moisture Products from GLEAM, GLDAS, and ERA5 Based on In Situ Observations and Triple Collocation Method over the Tibetan Plateau. *Journal of Hydrometeorology*, **23 (12)**, 1861–1878, https://doi.org/10.1175/JHM-D-22-0016.1.

Yang, Y., J. Zhang, Z. Bao, T. Ao, G. Wang, H. Wu, and J. Wang, 2021: Evaluation of Multi-Source Soil Moisture Datasets over Central and Eastern Agricultural Area of China Using In Situ Monitoring Network. *Remote Sensing*, **13 (6)**, 1175, https://doi.org/10.3390/rs13061175.

Yu, Z., G. Yang, S. Zuo, G. Jørgensen, M. Koga, and H. Vejre, 2020: Critical review on the cooling effect of urban blue-green space: A threshold-size perspective. *Urban Forestry & Urban Greening*, **49**, 126 630, https://doi.org/10.1016/j.ufug.2020.126630.

Zhang, S., and B. Wang, 2008: Global summer monsoon rainy seasons. *International Journal of Climatology*, **28 (12)**, 1563–1578, https://doi.org/10.1002/joc.1659.

Zhang, Y., and S. Fueglistaler, 2020: How Tropical Convection Couples High Moist Static Energy Over Land and Ocean. *Geophysical Research Letters*, **47 (2)**, https://doi.org/10.1029/2019GL086387.

Zhang, Y., I. Held, and S. Fueglistaler, 2021: Projections of tropical heat stress constrained by atmospheric dynamics. *Nature Geoscience*, **14 (3)**, 133–137, https://doi.org/10.1038/s41561-021-00695-3.

Zhao, W. L., and Coauthors, 2019: Physics-Constrained Machine Learning of Evapotranspiration. *Geophysical Research Letters*, **46 (24)**, 14 496–14 507, https://doi.org/10.1029/2019GL085291.

Zheng, X., and E. A. B. Eltahir, 1998: A Soil Moisture-Rainfall Feedback Mechanism: 2. Numerical experiments. *Water Resources Research*, **34 (4)**, 777–785, https://doi.org/10.1029/97WR03497.

Zhou, W., W. Cao, T. Wu, and T. Zhang, 2023: The win-win interaction between integrated blue and green space on urban cooling. *Science of The Total Environment*, **863**, 160 712, https://doi.org/10.1016/j.scitotenv.2022.160712.

Accepted for publication in *Journal of Climate*. DOI 10.1175/JCLI-D-23-0132.1.